Electronic Supplementary Information (ESI)

Pillar[5]arene-Based Tunable Luminescent Materials via Supramolecular Assembly-Induced Förster Resonance Energy Transfer Enhancement

*Nan Song,[a,c] Xin-Yue Lou,[a] Hao Yu,[a] Paul S. Weiss,[b] Ben Zhong Tang[c] and Ying-Wei Yang[a,]**

Table of Contents

Experimental Procedures

1. Materials and Methods

Materials. *p*-Hydroxyl anisole, paraformaldehyde $(CH_2O)_n$, potassium iodide (KI), and 1,4-dibromobutane were reagent grade and purchased from Aladdin Reagents (Shanghai, China) or Sigma-Aldrich (Darmstadt, Germany). Potassium carbonate (K_2CO_3) was obtained from J&K Co. Ltd. (Beijing, China). All of the solvents used in the study were reagent grade without further purification, purchased from commercial sources. H1-4C4P, H3-4C1P, H5-4CM and DSA-G were synthesized according to published methods.[S1-S4]

Methods. ^{1}H NMR spectra were recorded on a Bruker 300 MHz NMR spectrometer. ^{13}C NMR spectra were recorded on a Bruker 500 MHz NMR spectrometer. MALDI-TOF MS spectra were obtained from an autoflex TOF/TOF (Bruker, Germany) mass spectrometer, equipped with a nitrogen laser (337 nm, 3 ns pulse). The fluorescence microscopy images were obtained on an Olympus BX51 fluorescence microscopy. Fluorescence spectra were obtained on a Shimadzu RF-5301PC spectrofluorometer (the condition of the fluorescent measurements maintained the same as slit widths: ex. 5 nm, em. 5 nm, 25 ºC, without further notes). The time-resolved fluorescence decay curves and quantum yields were measured on a FLS920 instrument (Edinburgh Instrument, Britain). Quantum yields were calculated using an integrating sphere.

2. Syntheses and Characterization

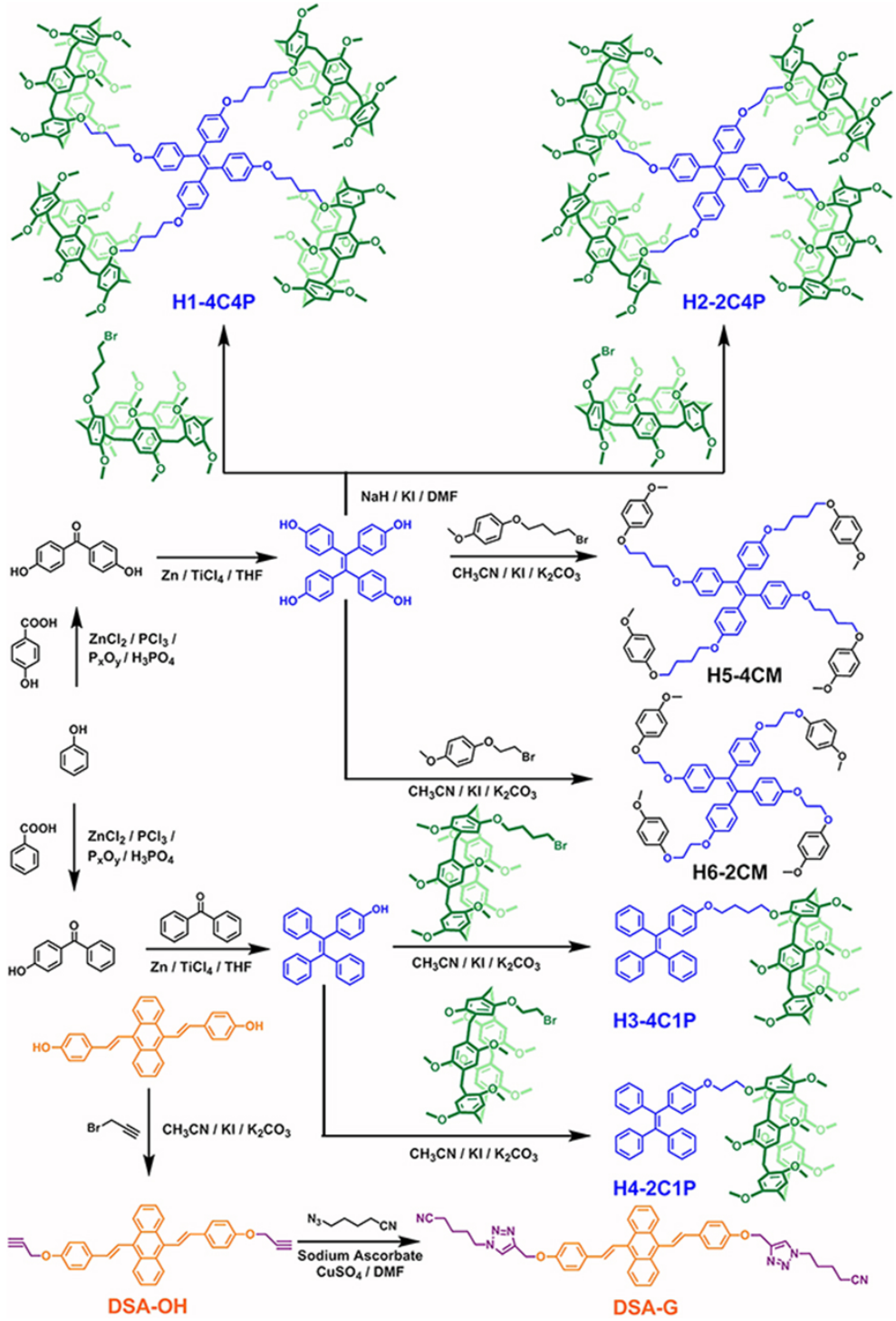

Figure S1. Synthetic route to all compounds. Synthetic route to **H1-4C4P, H2-2C4P, H3-4C1P**, **H4-2C1P**, **H5-4CM**, **H6-2CM**, and **DSA-G**.

2.1. Synthesis and Characterization of H2-2C4P

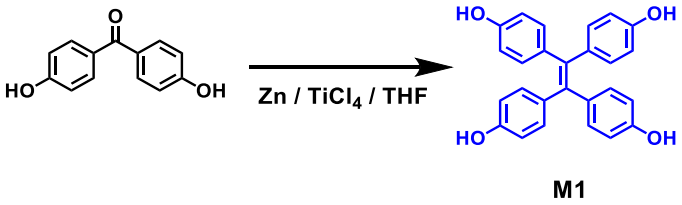

M1

Figure S2. Synthetic route to **M1**.

Synthesis of M1 (Tetrahydroxyl tetraphenylethene). (Figure S2) Tetrahydroxyl tetraphenylethene was synthesized through Cross McMurry reactions between two bis(4-hydroxyphenyl)-methanones. Zn powder (1.7 g, 25 mmol) was dispersed in dried THF (40 mL) under nitrogen atmosphere, and $TiCl_4$ (1.7 mL, 15 mmol) was added to the mixture dropwise after the temperature was cooled to 0 °C. The mixture was refluxed for 1.5 h and cooled to 0 °C again. Bis(4-hydroxyphenyl)methanones (1.07 g, 5 mmol) was dissolved into dried THF (15 mL) and the solution was added into the above mixture dropwise. After refluxing for 4 h, the reaction was quenched by the addition of a K_2CO_3 saturated solution. After filtration, the residue was washed with THF several times. The filtrate was concentrated via rotary evaporation, then extracted by ethyl acetate and dried with anhydrous Na_2SO_4. The crude material was purified by chromatography (silica gel, petroleum ether : EtOAc = 2:1) to give a final product with the yield of 350 mg (35%). 1H NMR (300 MHz, DMSO-d_6, 25 °C) δ (ppm): 9.222 (s, 4H), 6.699 (d, J = 6 Hz, 8H), 6.475 (d, J = 6 Hz, 8H).

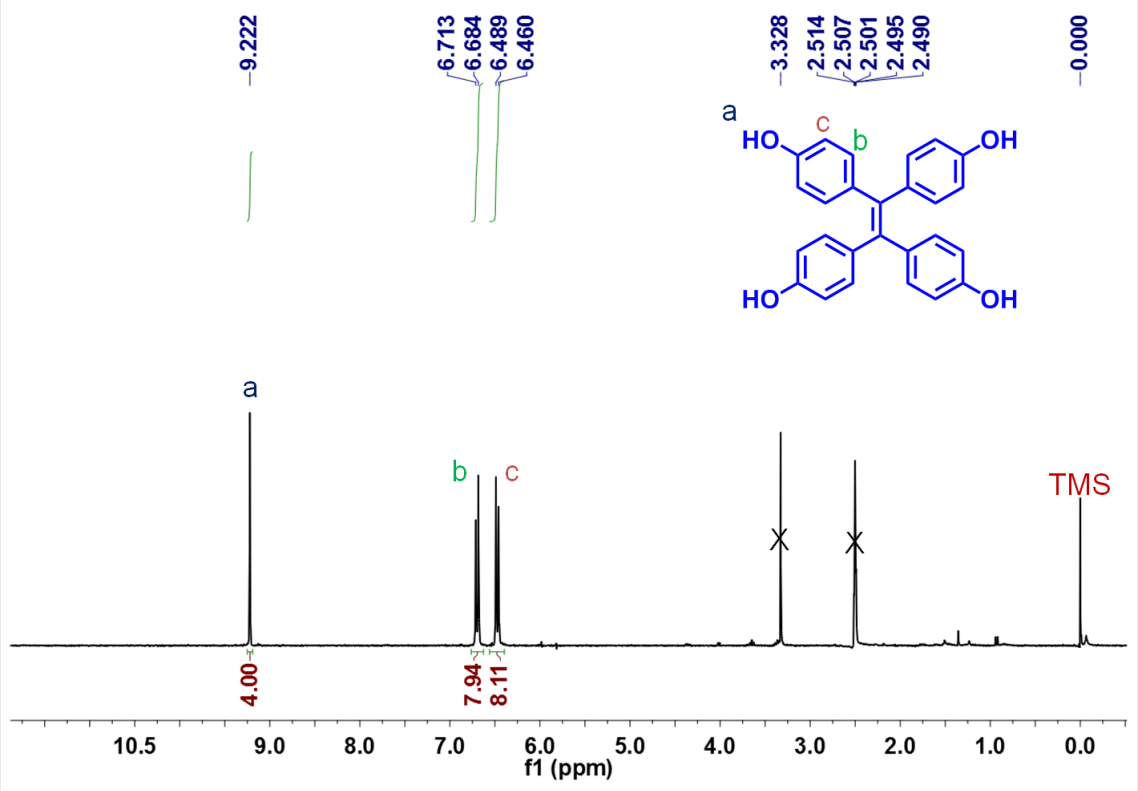

Figure S3. ^{1}H NMR spectrum of **M1.**

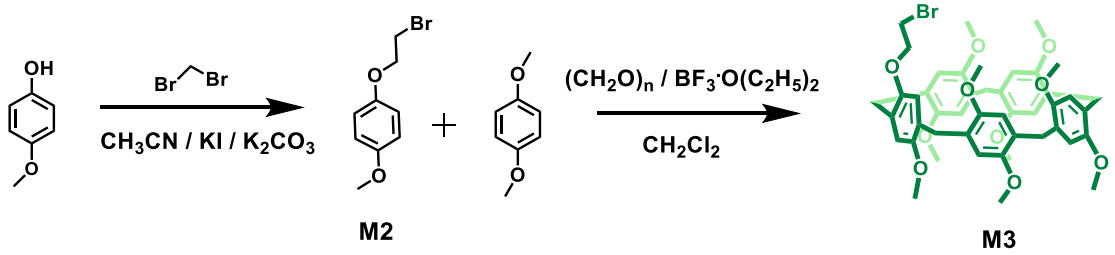

Figure S4. Synthetic route to **M3.**

Synthesis of M2. (Figure S4) 4-Methoxyphenol (9.3 g, 75 mmol) and K_2CO_3 (12.0 g, 90 mmol) were dispersed in 300 ml MeCN and the reaction was stirred for 30 min at room temperature. Then, 1,2-dichloroethane (9.8 mL, 115 mmol) and KI (100 mg) were added to the above solution and the mixture was refluxed at 85 °C for 10 h. After filtration, the filtrate was concentrated under vacuum and purified by chromatography (silica gel, petroleum ether : EtOAc = 20:1). The product was obtained after drying under vacuum. Yield: 2.9 g, 17%. 1H NMR (300 MHz, $CDCl_3$, 25 °C) δ (ppm): 6.855 (s, 4H), 4.248 (t, J = 6 Hz, 2H), 3.776 (s, 3H), 3.616 (d, J = 6 Hz, 2H).

Synthesis of M3. (Figure S4) M2 (0.468 g), 1,4-dimethoxybenzene (1.375 g) and paraformaldehyde (1.1 g) were dispersed in dried CH_2Cl_2 (90 mL) and the mixture was stirred for 20 min at room temperature. Then, $BF_3{\cdot}O(C_2H_5)_2$ (1.8 mL) was added into the mixture under the ice-water bath. The reaction was quenched with addition of water after stirred for 30 min. The mixture was extracted with Na_2CO_3 solution, water and brine, respectively. The crude product was purified by chromatography after concentration (silica gel, petroleum ether : CH_2Cl_2 EtOAc = 90:30:1). Then, the final white product was obtained. Yield: 100 mg, 6%. 1H NMR (300 MHz, $CDCl_3$, 25 °C) δ (ppm): 6.769 (m, 10H), 4.033 (t, J = 6 Hz, 2H), 3.777 (s, 10H), 3.673 (m, 27H), 3.436 (t, J = 6 Hz, 2H).

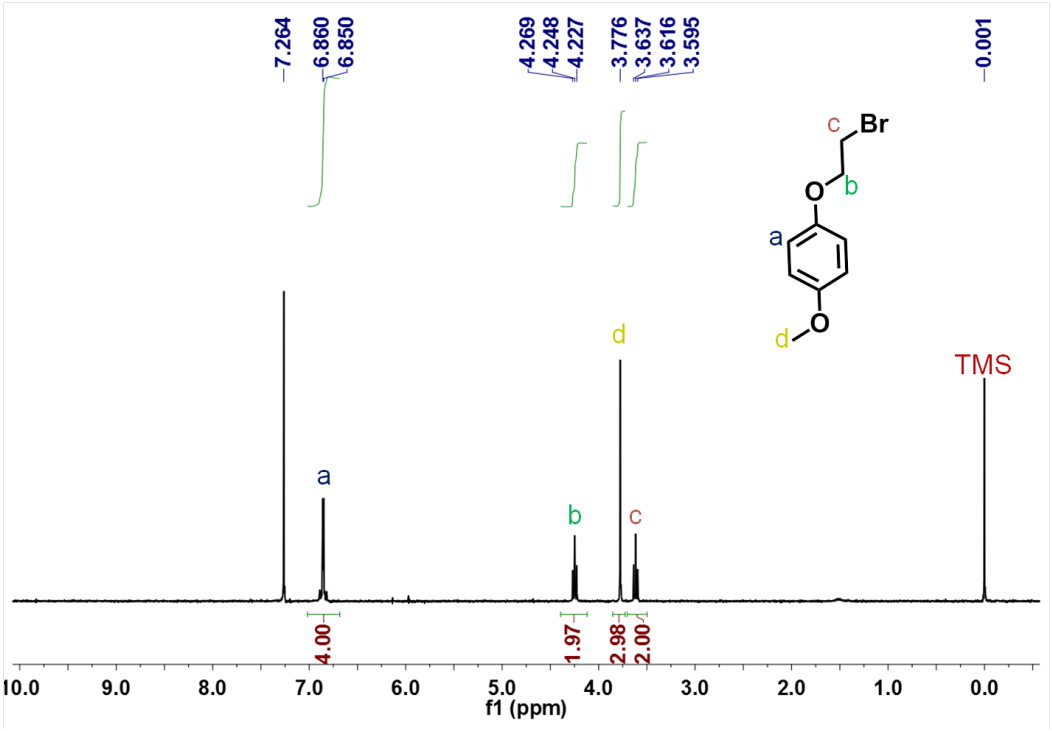

Figure S5. ^{1}H NMR spectrum of **M2**.

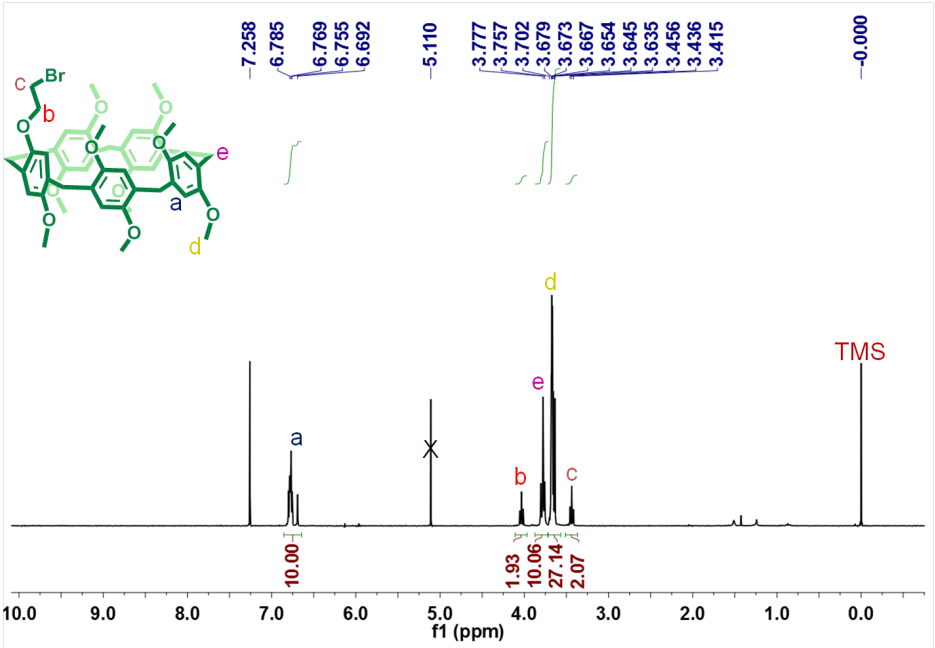

Figure S6. ^{1}H NMR spectrum of **M3**.

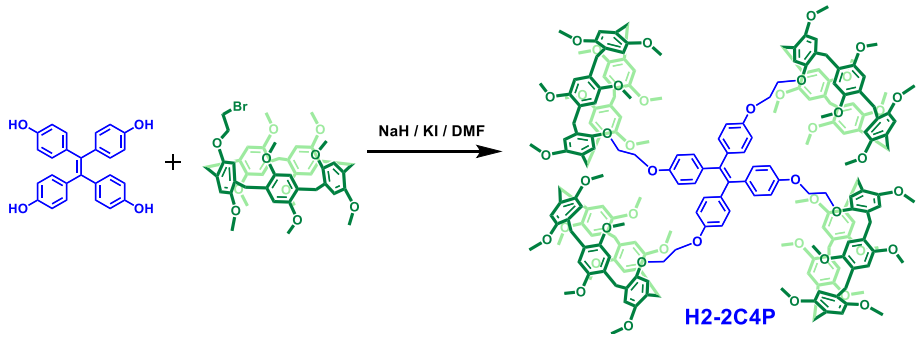

Figure S7. Synthetic route to **H2-2C4P**.

Synthesis of H2-2C4P.[S1] (Figure S7) Tetrahydroxyl tetraphenylethene (130 mg, 0.33 mmol) was dispersed in anhydrous DMF (40 mL) under nitrogen atmosphere. Then, NaH (40 mg, 1.64 mmol), KI (10 mg) and M3 (1.4 g, 1.64 mmol) were added. After reacting at 90 °C for 40 h under nitrogen atmosphere, the mixture was poured into brine (100 mL) and extracted with EtOAc for three times. The organic layers were collected, then washed with water and brine several times each. The organic layer was dried with anhydrous Na_2SO_4 and concentrated under rotary evaporation. The residue was purified by chromatography (silica gel, petroleum ether : EtOAc = 5:1 to 2:1) and dried under vacuum to give a yellow product. Yield: 330 mg, 29%. ^{1}H NMR (300 MHz, $CDCl_3$, 25 °C) δ (ppm): 6.962 (d, J = 9 Hz, 8H), 6.779-6.732 (m, 40H), 6.701 (d, J = 9 Hz, 8H), 4.132 (t, 8H), 4.059 (t, 8H), 3.765 (s, 40H), 3.653-3.509 (m, 108H). ^{13}C NMR (125 MHz, $CDCl_3$, 25 °C) δ (ppm): 157.2, 151.2, 150.8, 149.7, 138.4, 137.1, 132.6, 129.0, 128.2, 115.9, 114.1, 113.7, 67.7, 66.8, 55.7, 29.7. MALDI-TOF: Calculated for $C_{210}H_{220}O_{44}$ [M]: 3445.498, $[M+Na]^+$: 3468.487, Found: [M]: 3445.243, $[M+Na]^+$: 3468.487.

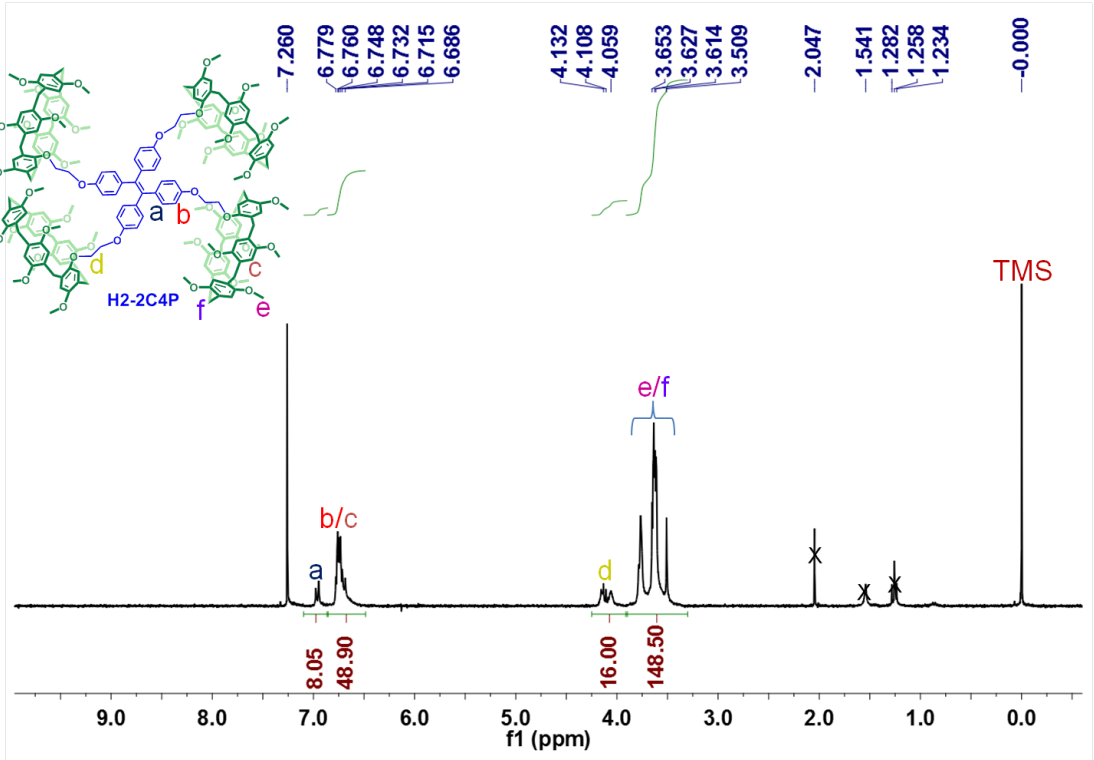

Figure S8. ^{1}H NMR spectrum of **H2-2C4P**.

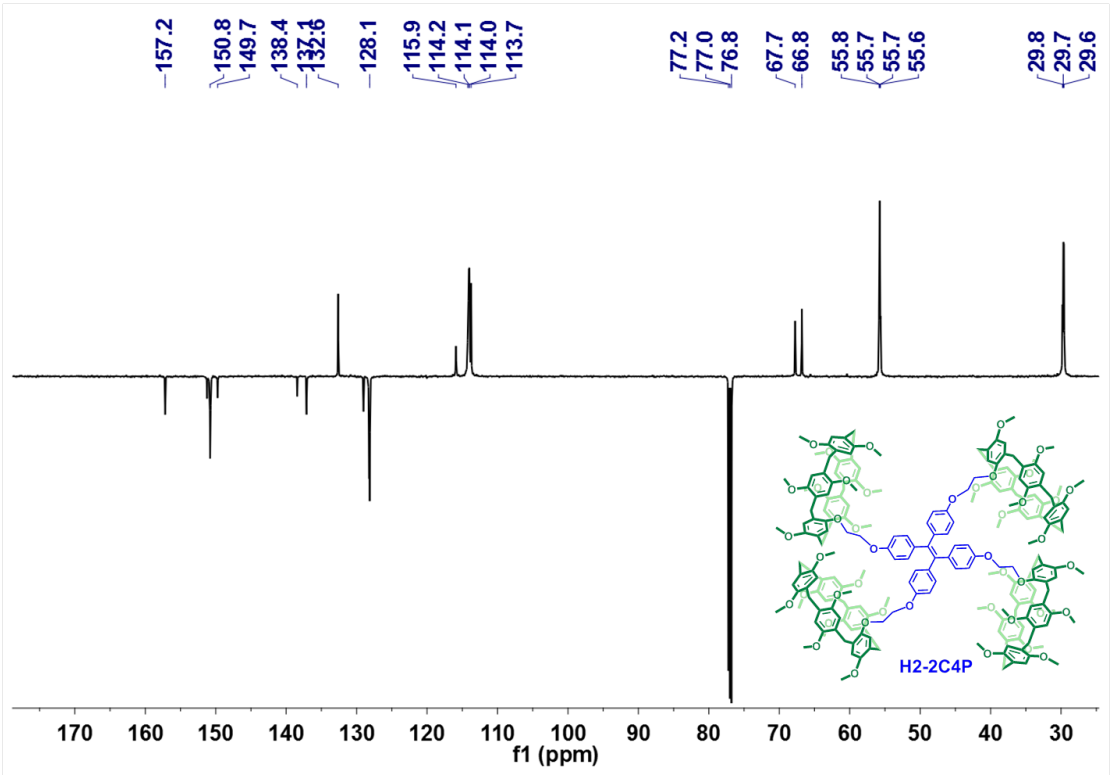

Figure S9. ^{13}C NMR spectrum of **H2-2C4P**.

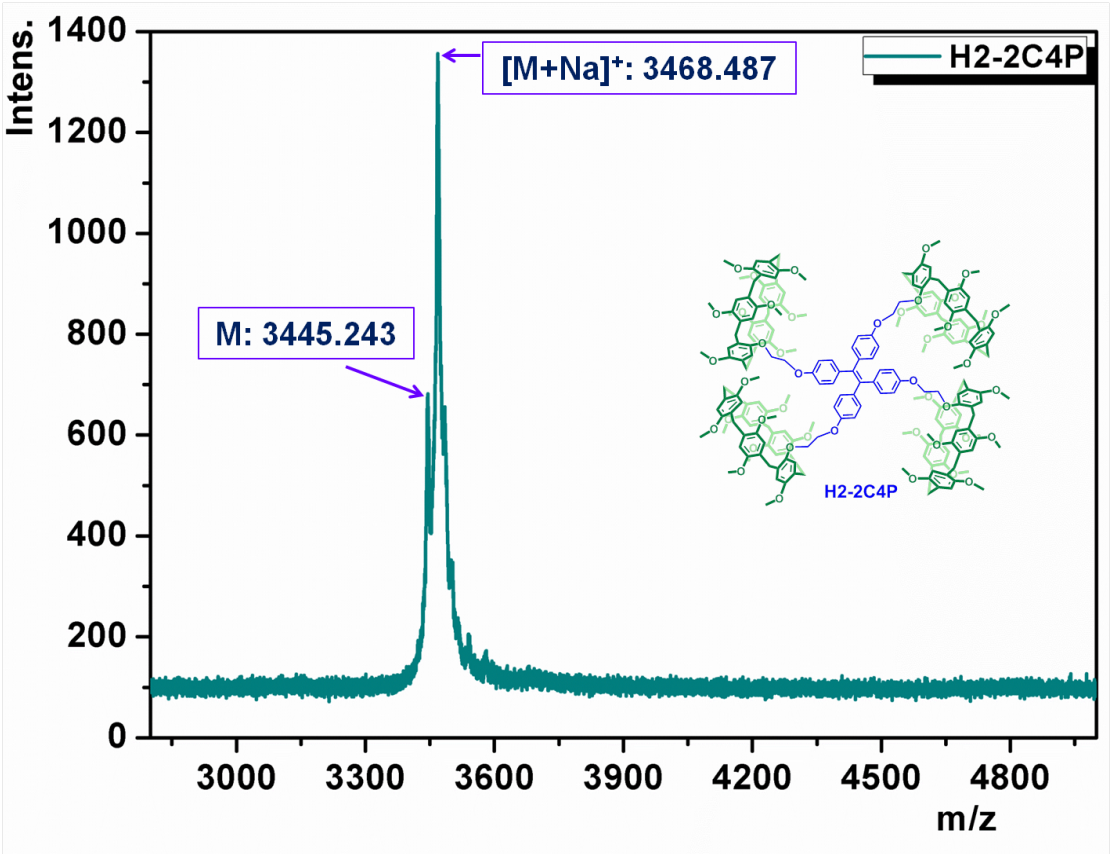

Figure S10. MALDI-TOF spectrum of **H2-2C4P**.

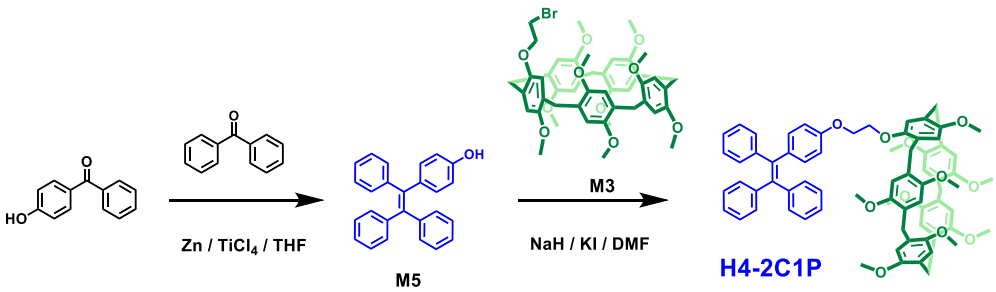

Figure S11. Synthetic route to **H4-2C1P**.

2.2. Synthesis and Characterization of H4-2C1P

Synthesis of H4-2C1P. (Figure S11) M5 was synthesized according to the literature methods.[1] Under a nitrogen atmosphere, Zn powder (1.7 g, 25 mmol) was dispersed in THF (40 mL) and $TiCl_4$ (1.7 mL, 15 mmol) was added dropwise after the mixture was cooled to 0 °C. The mixture was refluxed and stirred for 1.5 h. Then, the mixture was cooled to 0 °C, a solution of diphenyl ketone (0.455 g, 2.5 mmol) and *p*-hydroxyl diphenyl ketone (0.495 g, 2.5 mmol) in THF (15 mL) was added slowly to the above mixture and heated at reflux until

the carbonyl compounds were consumed, which was detected with TLC. The reaction was quenched with 10% K_2CO_3 aqueous solution and extracted with CH_2Cl_2. The organic layer was collected and concentrated. The crude material was purified by chromatography (silica gel, *n*-hexane : CH_2Cl_2 : acetone = 20:5:1) to give a white product. Yield: 22%. M5 (80 mg, 0.2 mmol) and K_2CO_3 (0.5 g) were dispersed in MeCN (60 mL) and the mixture was stirred for 30 min at room temperature. Then KI and M3 (180 mg, 0.2 mmol) were added into the mixture and the mixture was refluxed for 40 h under nitrogen atmosphere. The crude residue was filtered and washed with chloroform after cooling down. The filtrate was concentrated, and subjected to column chromatography (silica gel, EtOAc : *n*-hexane = 1:20, 1:10, 1:5), white product was obtained. Yield: 110 mg, 50%. ^{1}H NMR (300 MHz, $CDCl_3$, 25 °C) δ (ppm): 7.093 (m, 15H), 6.933 (d, 2H), 6.758 (m, 10H), 6.683 (d, 2H), 4.141 (t, 4H), 3.774 (s, 10H), 3.648 (m, 27H).

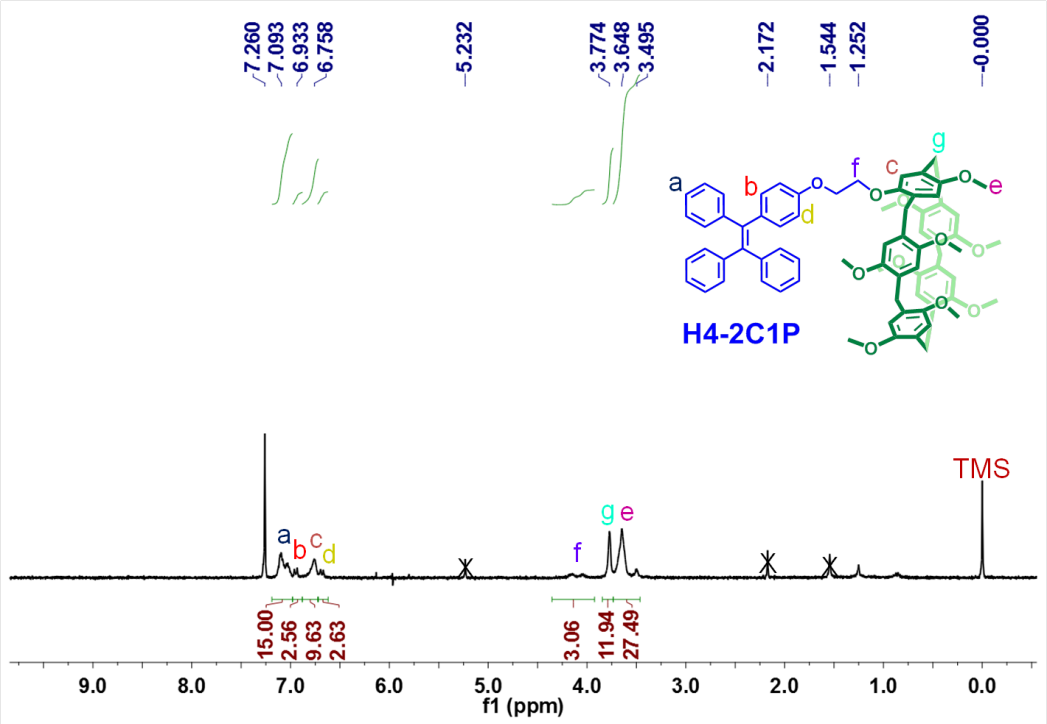

Figure S12. ^{1}H NMR spectrum of **H4-2C1P**.

2.3. Synthesis and Characterization of H6-2CM

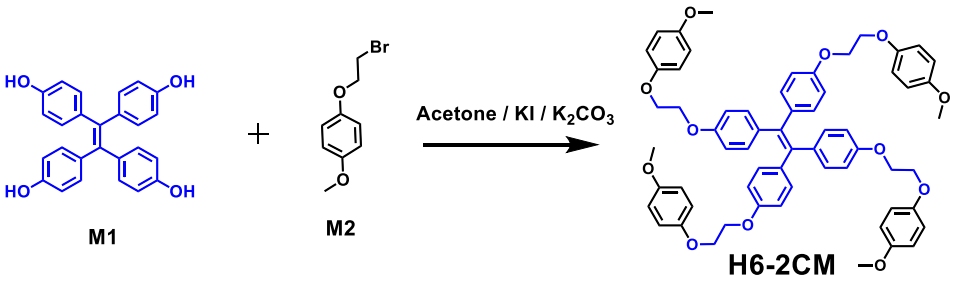

Figure S13. Synthetic route to **H6-2CM**.

Synthesis of H6-2CM. (Figure S13) **H6-2CM** was also synthesized according to a modified literature procedure.[S1] M1 (50 mg, 0.125 mmol) was dispersed in acetone (50 mL) and K_2CO_3 (1 g), a small amount of 18-crown-6 were added. The mixture was stirred for 30 min at room temperature. KI (10 mg) and M2 (175 mg, 0.75 mmol) were added into the above mixture. The mixture was refluxed for 4 days under a nitrogen atmosphere. The mixture was filtered and washed with chloroform after cooling down. The filtrate was collected and concentrated, the residue was subjected to column chromatography (silica gel, petroleum ether : EtOAc = 10:1), the white product (72 mg) was obtained. Yield: 65%. ^{1}H NMR (300 MHz, $CDCl_3$, 25 °C) δ (ppm): 6.906 (m, 24H), 6.703 (m, 8H), 4.239 (s, 16H), 3.769 (s, 12H).

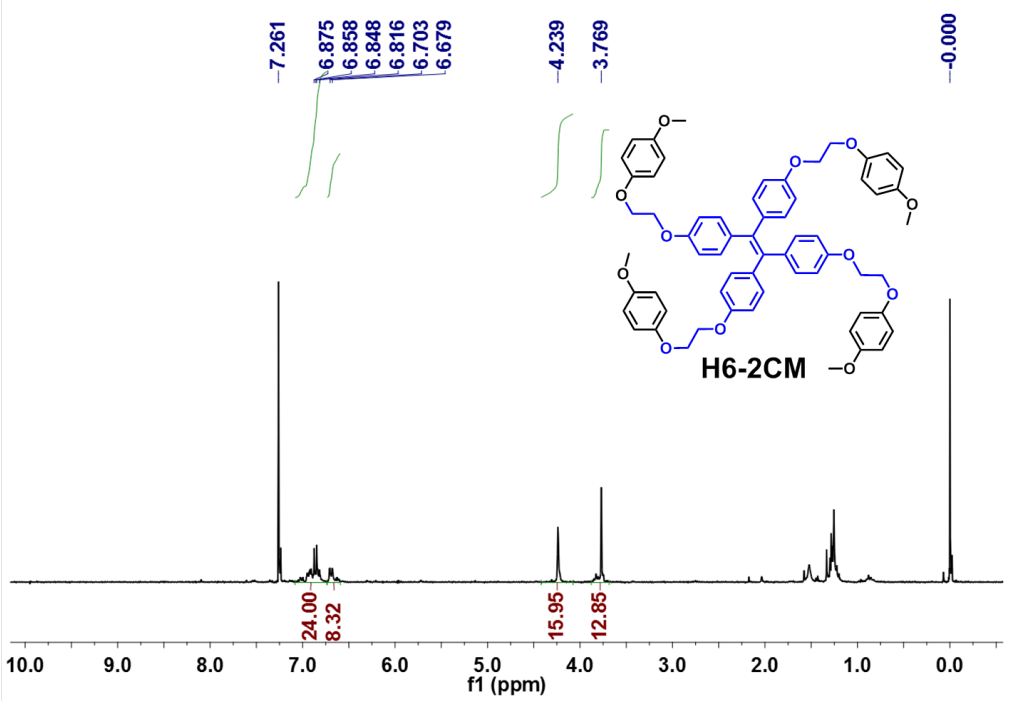

Figure S14. ^{1}H NMR spectrum of **H6-2CM**.

3. Aggregation-Induced Emission of H2-2C4P

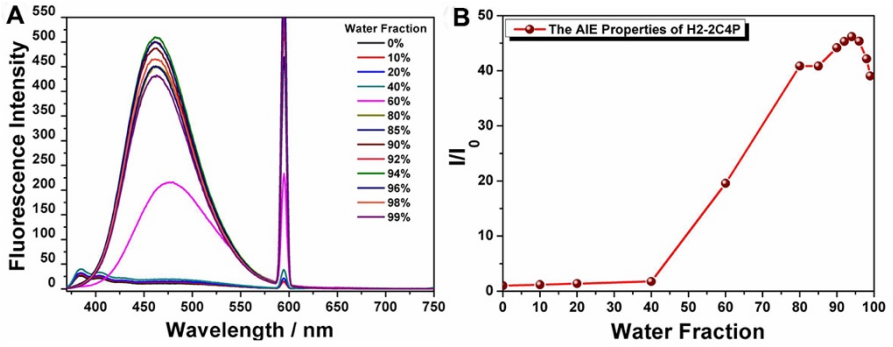

Figure S15. Aggregation-induced emission of **H2-2C4P**. (A) Fluorescence emission spectra of **H2-2C4P** in mixed solvents of THF/H_2O with the volume fractions of water varying in the range of 0-99% (λ_{ex} = 295 nm, λ_{em} = 456 nm; slit widths: ex. 3 nm, em. 3 nm; 25 ºC; concentration: [**H1-4C4P**] = 1.0 μM); (B) Plot of the fluorescent intensity of **H2-2C4P** at 456 nm *vs* the composition of the THF/H_2O mixture (water fraction).

4. Aggregation-Induced Emission of DSA-G

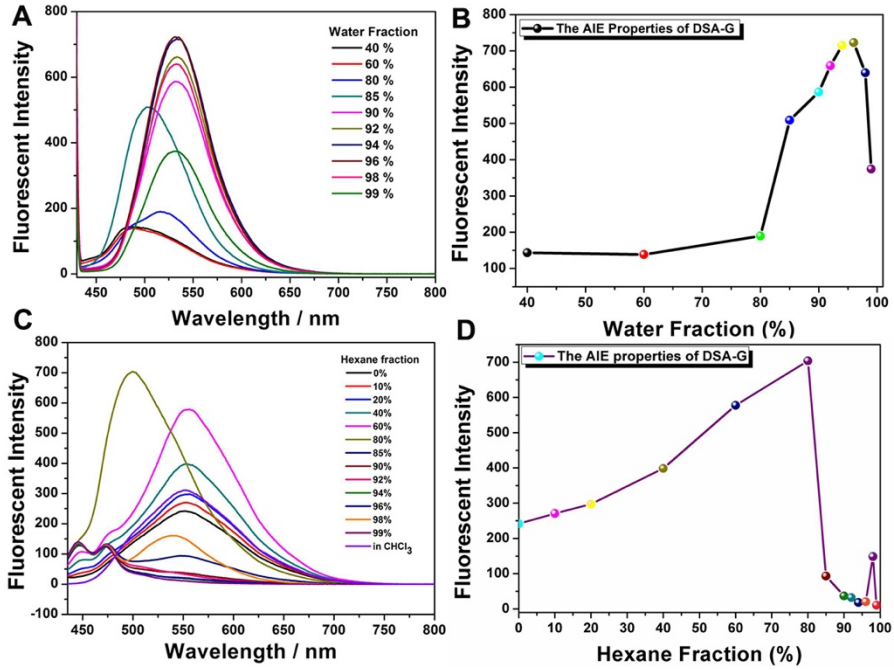

Figure S16. Aggregation-induced emission of **DSA-G**. Fluorescence emission spectra of DSA-G in the mixed solvents of (A) THF/H_2O with the volume fractions of water varying in the range of 0-99% and (C) $CHCl_3$/Hexane (λ_{ex} = 415 nm, λ_{em} = 553 nm; slit widths: ex. 10 nm, em. 10 nm; 25 ºC; concentration: [DSA-G] = 1.0 μM); Plot of the fluorescent intensity of DSA-G at 553nm *vs* the composition of the (B) THF/H_2O mixture (water fraction) and (D) $CHCl_3$/hexane mixture (hexane fraction).

5. UV-Vis and Fluorescence Experiments in Solvents

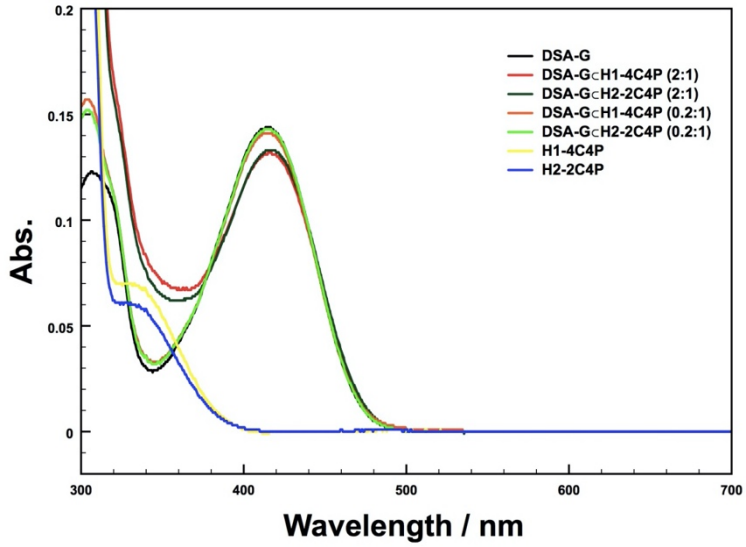

Figure S17. UV-Vis experiments of different host/guest ratio. UV-Vis spectra of **DSA-G⊂H1-4C4P** and **DSA-G⊂H2-2C4P** with molar ratios of 2:1 and 0.2:1 (control experiments: individual **H1-4C4P**, **H2-2C4P** and **DSA-G**.

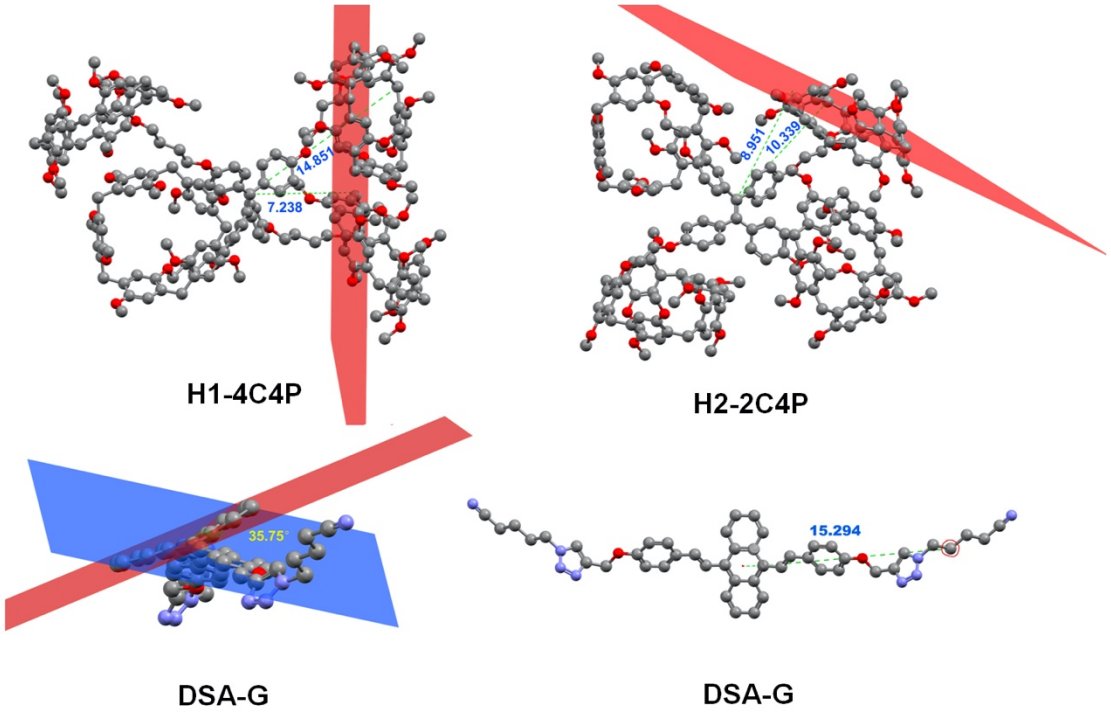

Figure S18. Molecular modeling of H1-4C4P, H2-2C4P, and DSA-G with energy minimization, respectively, using ChemDraw 3D.

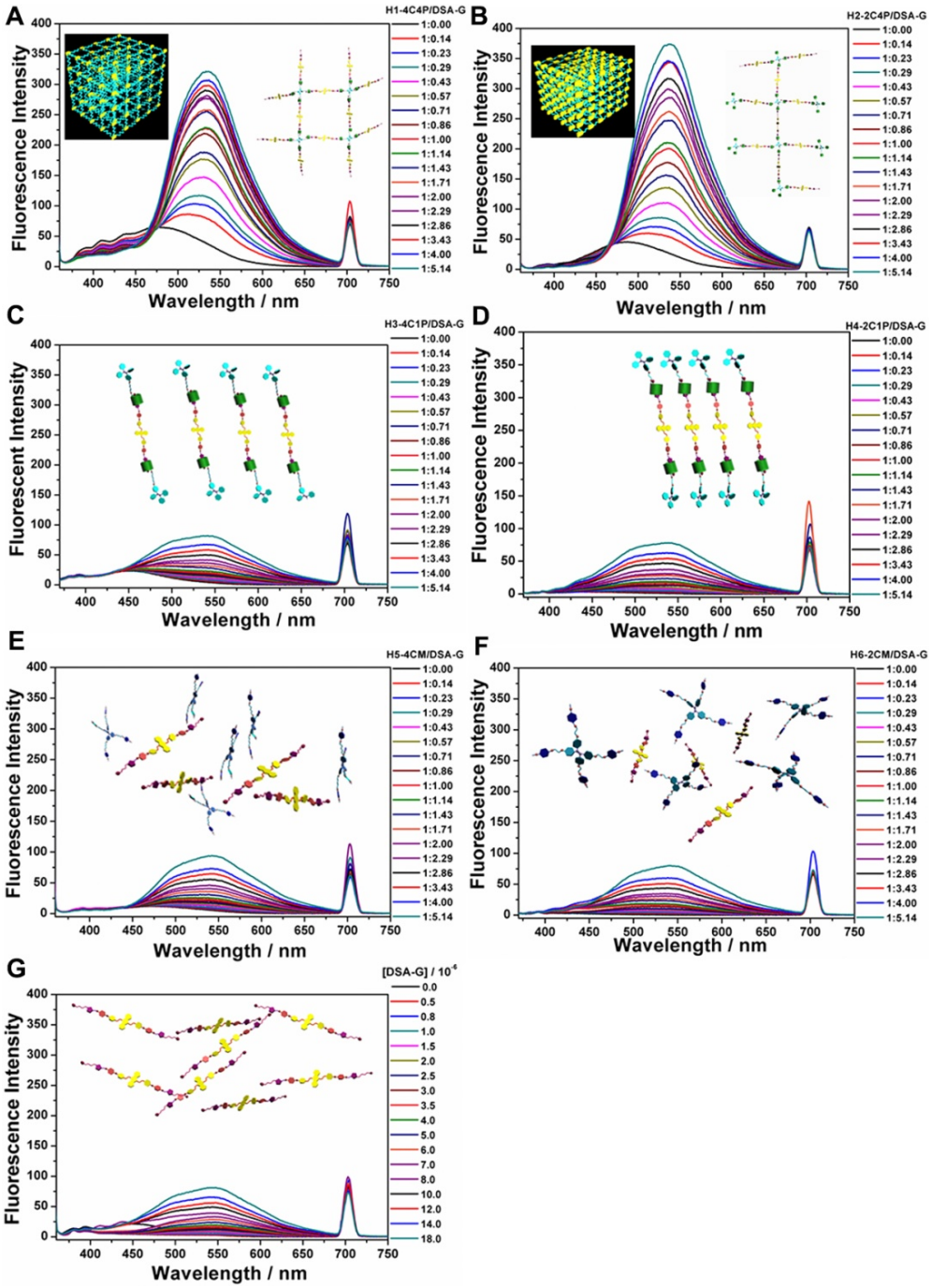

Figure S19. Fluorescence experiments in solvents. Fluorescence emission spectra of (A) **DSA-G⊂H1-4C4P**; (B) **DSA-G⊂H2-2C4P**; (C) **DSA-G⊂H3-4C1P**; (D) **DSA-G⊂H4-2C1P**; (E) **H5-4CM/DSA-G**; (F) **H6-2CM/DSA-G**; (G) **DSA-G**; (λ_{ex} = 350 nm; slit widths: ex. 5 nm, em. 5 nm; 25 ºC; concentration: [**H1-4C4P**] = [**H2-2C4P**] = [**H3-4C1P**] = [**H4-2C1P**] = [**H5-4CM**] = [**H6-2CM**] = 3.5 μM; [**DSA-G**] = 0 μM, 0.5 μM, 0.8 μM, 1.0 μM, 1.5 μM, 2.0 μM, 2.5 μM, 3.0 μM, 3.5 μM, 4.0 μM, 5.0 μM, 6.0 μM, 7.0 μM, 8.0 μM, 10.0 μM, 12.0 μM, 14.0 μM, 18.0 μM); (G) Plots of fluorescence emission changes of **DSA-G⊂H1-4C4P** (black), **DSA-G⊂H2-2C4P** (red), **DSA-G⊂H3-4C1P** (blue), **DSA-G⊂H4-2C1P** (dark cyan), **H5-4CM/DSA-G** (magenta), **H6-2CM/DSA-G** (dark yellow), **DSA-G** (navy) at λ_{em} = 535 nm.

6. Quantum Yields and Time-Resolved Fluorescence Decay Curves

Table S1. Quantum yields and time-resolved fluorescence decay curves

	sn1	sn2	sn3	sn4	sn5	sn6	sn7
ϕ(%)	3.57	10.29	19.79	3.55	0.57	20.88	5.69
lf(ns)	0.44	1.52	1.87	1.31	0.26	1.68	1.44
k_r (s^{-1})	$8.14x10^7$	$6.76x10^7$	$1.06x10^8$	$2.71x10^7$	$2.22x10^7$	$1.24x10^8$	$3.94x10^7$
K_{nr}(s^{-1})	$2.19x10^9$	$5.90x10^8$	$4.29x10^8$	$7.36x10^8$	$3.88x10^9$	$4.71x10^8$	$6.54x10^8$

Parameters of quantum yields, fluorescence lifetimes, rate constants of radiative deactivation and non-radiative deactivation, relatively (sn1: **H1-4C4P** ([**H1-4C4P**] = 50 μM); sn2: **DSA-G** ([**DSA-G**] = 100 μM); sn3: **DSA-G⊂H1-4C4P** ([**H1-4C4P**] = 50 μM, [**DSA-G**] = 100 μM); sn4: **DSA-G⊂H3-4C1P** ([**H3-4C1P**] = 200 μM, [**DSA-G**] = 100 μM); sn5: **H2-2C4P** ([**H2-4C4P**] = 50 μM); sn6: **DSA-G⊂H2-2C4P** ([**H2-2C4P**] = 50 μM, [**DSA-G**] = 100 μM); sn7: **DSA-G⊂H4-2C1P** ([**H4-2C1P**] = 200 μM, [**DSA-G**] = 100 μM); quantum yields were measured using an integrating sphere.

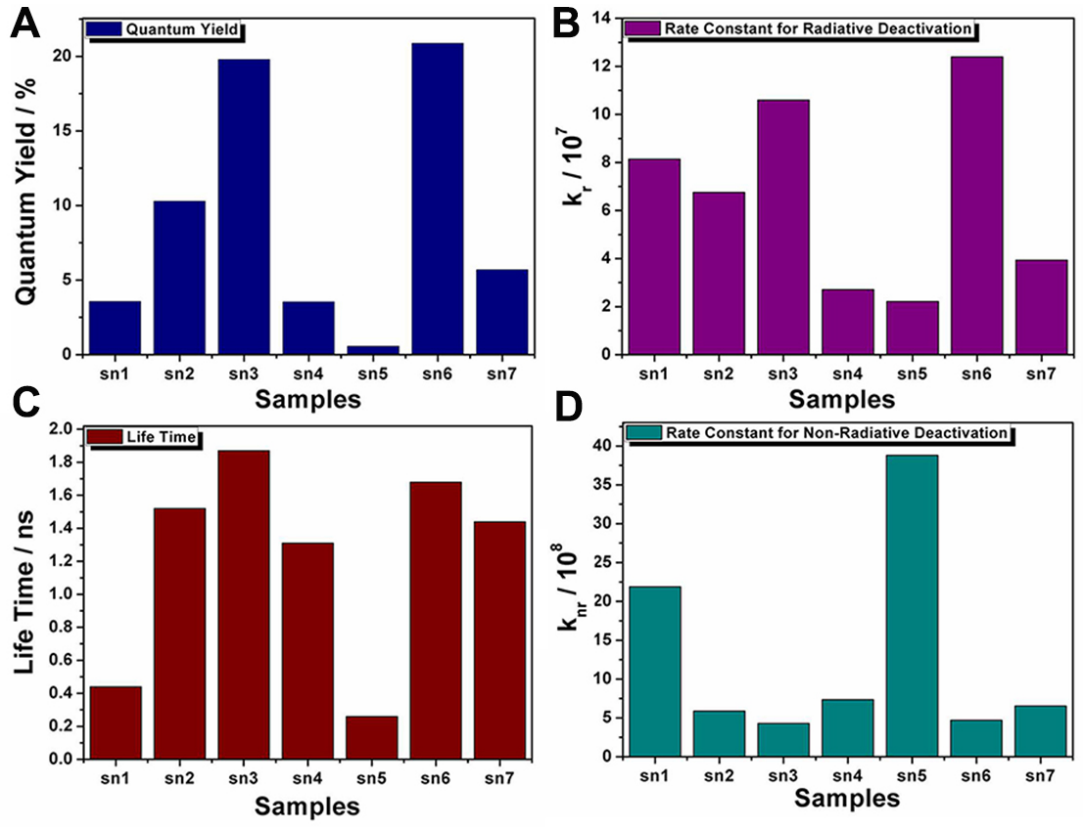

Figure S20. Quantum yields and time-resolved fluorescence decay curves. Histograms of (A) quantum yields, (B) rate constants of radiative deactivation, (C) fluorescence lifetimes and (D) rate constants of non-radiative deactivation about sn1-sn7 (sn1-sn7 are the same as mentioned in above table S1).

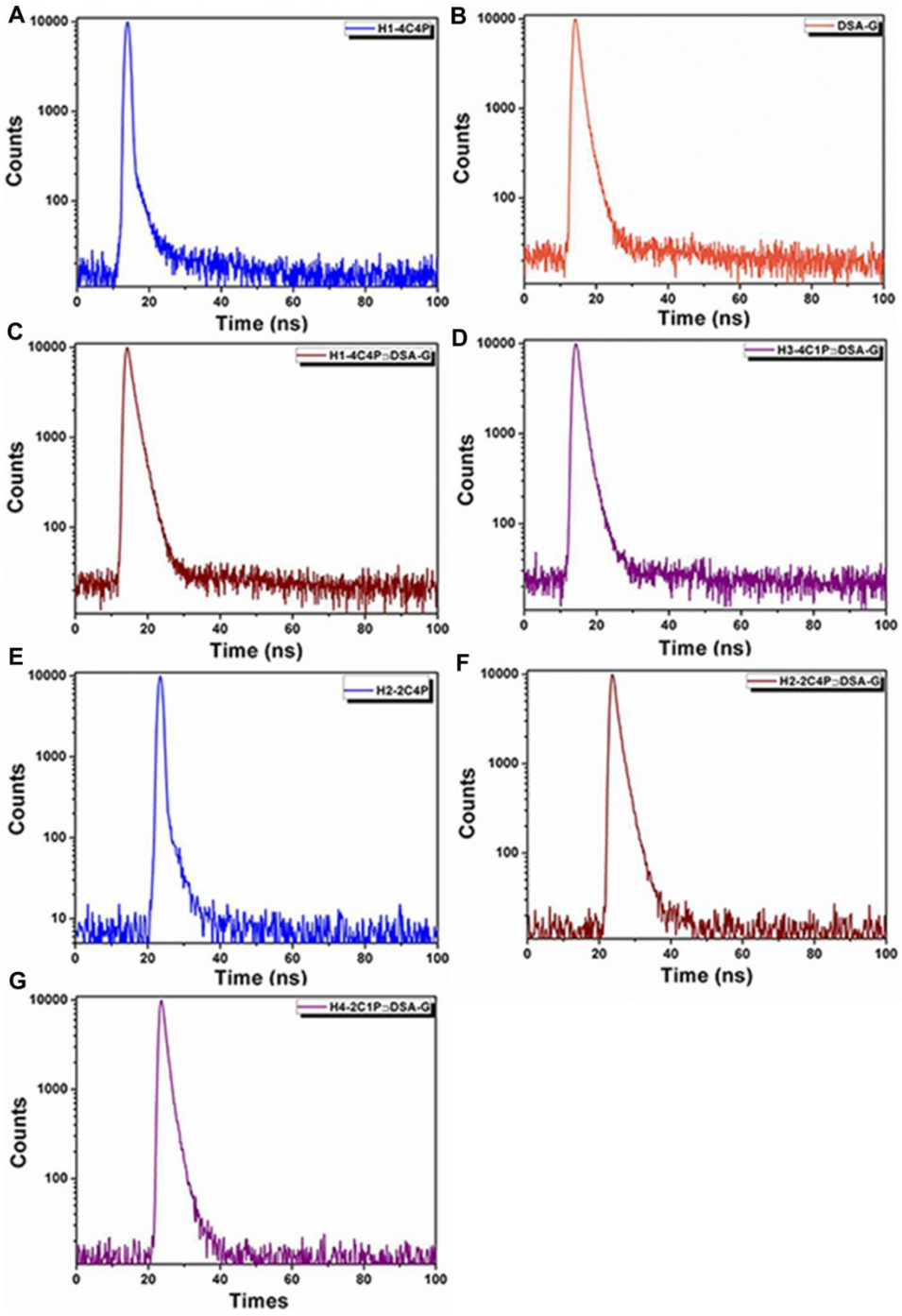

Figure S21. Time-resolved fluorescence decay curves. Time-resolved fluorescence decay curves of (A) **H1-4C4P** ([**H1-4C4P**] = 50 μM), (B) **DSA-G** ([**DSA-G**] = 100 μM), (C) **DSA-G⊂H1-4C4P** ([**H1-4C4P**] = 50 μM, [**DSA-G**] = 100 μM), (D) **DSA-G⊂H3-4C1P** ([**H3-4C1P**] = 200 μM, [**DSA-G**] = 100 μM), (E) **H2-2C4P** ([**H2-4C4P**] = 50 μM), (F) **DSA-G⊂H2-2C4P** ([**H2-2C4P**] = 50 μM, [**DSA-G**] = 100 μM), (G) **DSA-G⊂H4-2C1P** ([**H4-2C1P**] = 200 μM, [**DSA-G**] = 100 μM).

7. Stimuli-Responsiveness to Temperature and Solvents

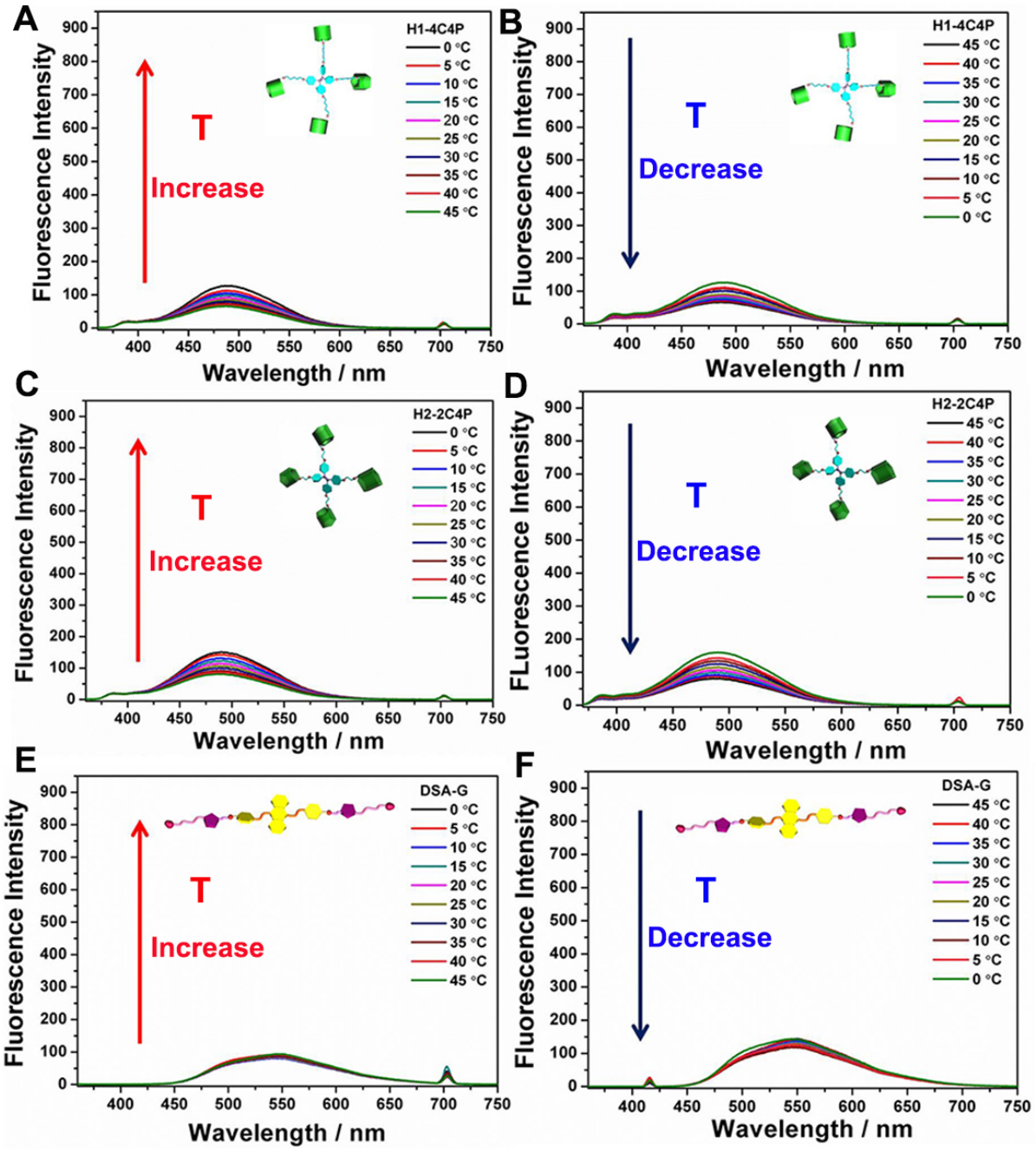

Figure S22. Stimuli-responsiveness to temperature of controlled experiments. Controlled experiments of thermo-responsiveness. Fluorescence emission spectra of **H1-4C4P** (A) upon elevating the temperature and (B) lowering the temperature, **H2-2C4P** (C) upon elevating the temperature and (D) lowering the temperature, **DSA-G** (E) upon elevating the temperature and (F) lowering the temperature (λ_{ex} = 350 nm; slit widths: ex. 3 nm, em. 5 nm; 25 ºC; concentration: [**H1-4C4P**] = [**H2-2C4P**] = 35 μM, [**DSA-G**] = 70 μM).

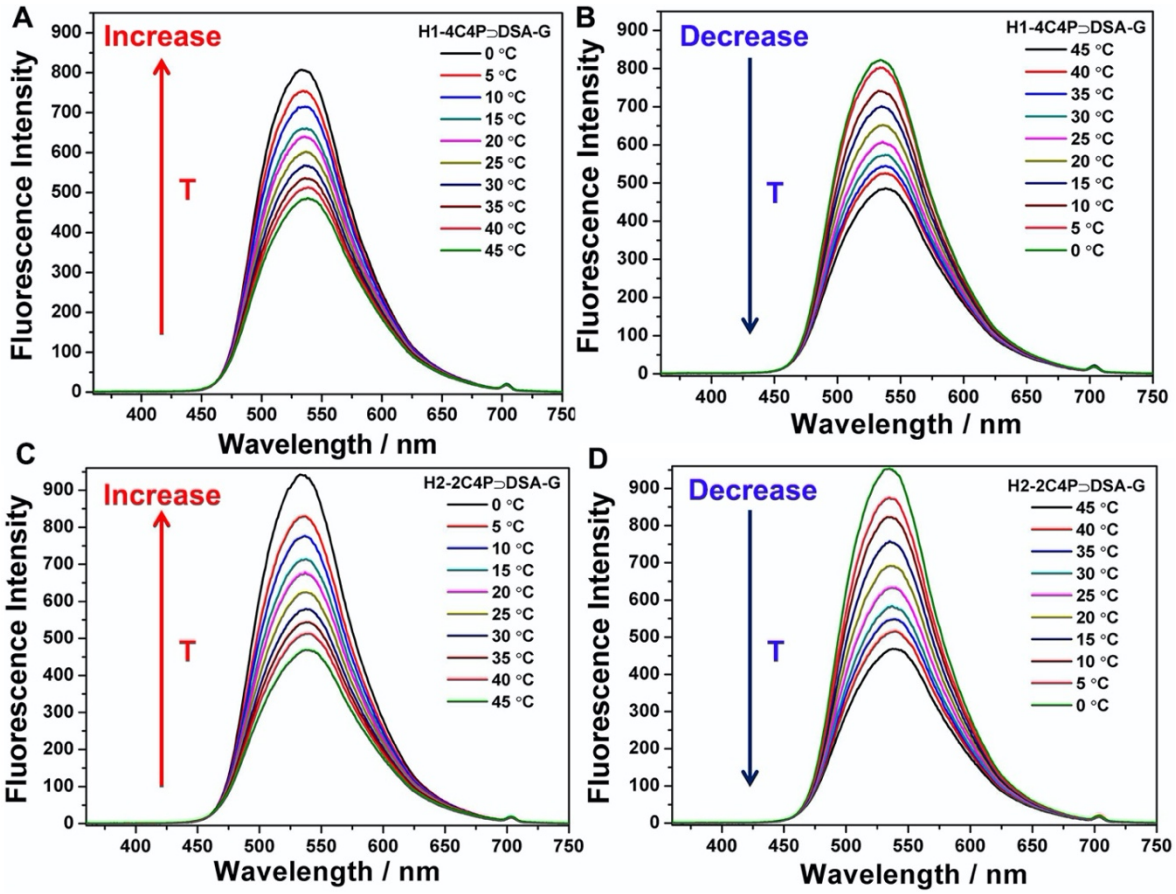

Figure S23. Stimuli-responsiveness to temperature. Fluorescence emission spectra of **DSA-G⊂H1-4C4P** (A) upon elevating the temperature and (B) lowering the temperature. Fluorescence emission spectra of **DSA-G⊂H2-2C4P** (C) upon elevating the temperature and (D) lowering the temperature (λ_{ex} = 350 nm; slit widths: ex. 3 nm, em. 5 nm; 25 ºC; concentration: [**H1-4C4P**] = [**H2-2C4P**] = 35 μM, [**DSA-G**] = 70 μM).

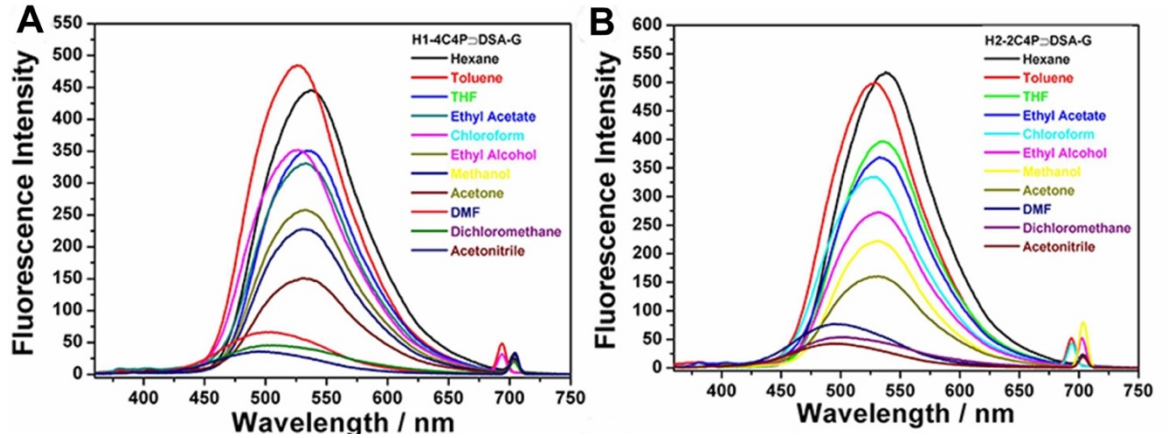

Figure S24. Stimuli-responsiveness to solvents. Fluorescent intensity spectra of (A) **DSA-G⊂H1-4C4P** and (B) **DSA-G⊂H2-2C4P** with the addition of different solvents (λ_{ex} = 350 nm; slit widths: ex. 3 nm, em. 5 nm; 25 ºC; concentration: [**H1-4C4P**] = [**H2-2C4P**] = 14 μM, [**DSA-G**] = 28 μM; all of the solvents are mixed with chloroform in the volume ratio of 1:1 to guarantee the solubility.).

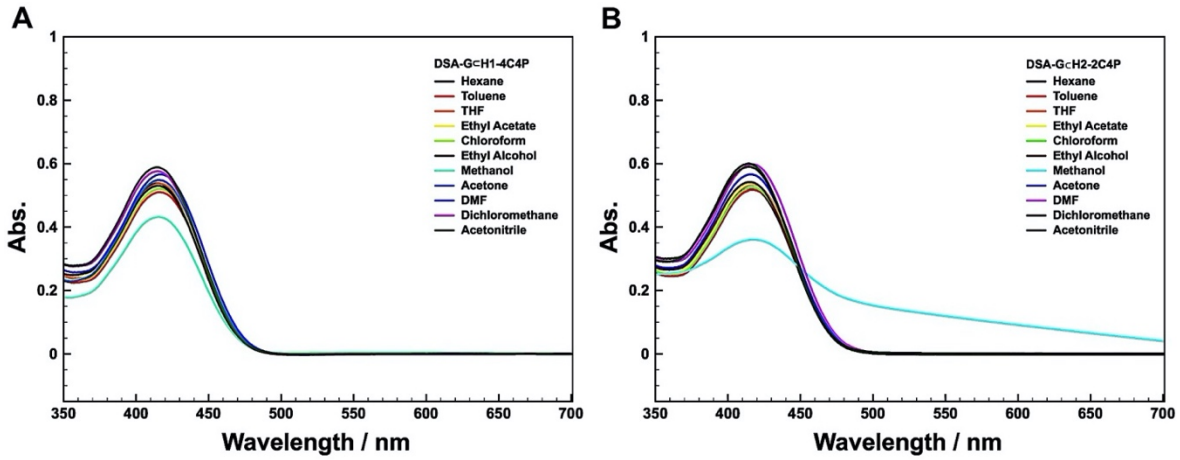

Figure S25. UV-Vis experiments in different solvents. UV-Vis spectra of (A) **DSA-G⊂H1-4C4P and (B) DSA-G⊂H2-2C4P** in various solvents (25 ºC; concentration: [**H1-4C4P**] = 3.5 μM, [**H2-2C4P**] = 3.5 μM, [**DSA-G**] = 7 μM; all the solvents are mixed with $CHCl_3$ in a volume ratio of 1:1 to guarantee solubility).

Table S2. Quantum Yields and Time-Resolved Fluorescence Decay Curves

Solvent	$\boldsymbol{\Phi}_f$ (%)	$\boldsymbol{\tau}$ (ns)	k_r ($s^{-1}\times10^7$)	k_{nr} ($s^{-1}\times10^7$)
Hexane	29.44	3.774	7.8	18.7
Toluene	32.59	1.875	17.4	35.9
THF	21.88	1.792	12.2	43.6
Ethyl Acetate	23.67	1.754	13.5	43.5
Chloroform	28.17	1.766	15.9	40.7
Ethanol	18.80	2.025	9.3	40.1
Methanol	16.88	2.112	8.0	39.4
Acetone	10.59	1.585	6.7	56.4
DMF	4.35	1.149	3.8	83.2
Dichloromethane	3.42	1.428	2.4	67.6
Acetonitrile	2.61	1.151	2.3	84.6

Parameters of quantum yields, fluorescence lifetimes, rate constants of radiative deactivation and non-radiative deactivation **of DSA-G⊂H1-4C4P** in different solvents ([**H1-4C4P**] = 50 μM, [**DSA-G**] = 100 μM).

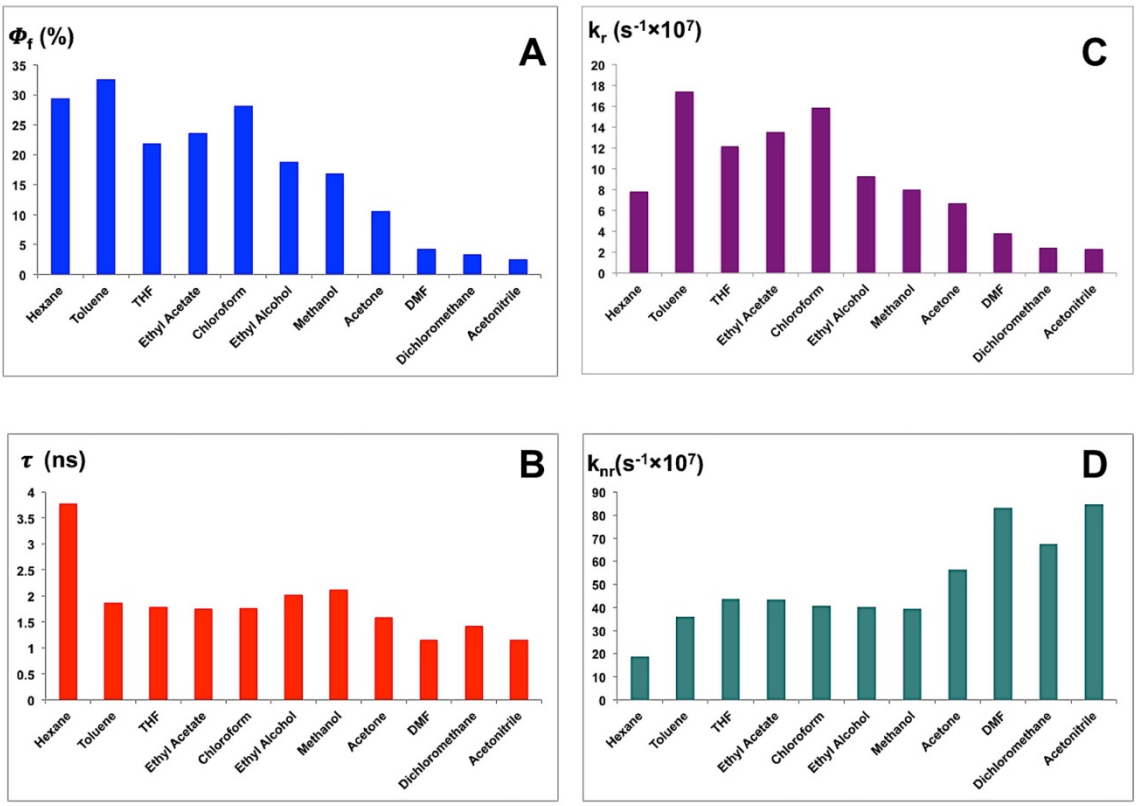

Figure S26. Quantum yields and time-resolved fluorescence decay curves. Histograms of (A) quantum yields, (B) rate constants of radiative deactivation, (C) fluorescence lifetimes and (D) rate constants of non-radiative deactivation of **DSA-G⊂H1-4C4P** in different solvents ([**H1-4C4P**] = 50 μM, [**DSA-G**] = 100 μM, as shown in Table S2).

Table S3. Quantum Yields and Time-resolved Fluorescence Decay Curves

Solvent	Φ_f (%)	τ (ns)	k_r ($s^{-1}\times10^7$)	k_{nr} ($s^{-1}\times10^7$)
Hexane	33.74	1.974	17.1	33.6
Toluene	35.54	1.936	18.5	33.3
THF	25.89	1.673	15.5	44.3
Ethyl Acetate	26.64	1.670	15.9	43.9
Chloroform	29.05	1.647	17.6	43.1
Ethanol	19.99	1.645	12.2	48.6
Methanol	27.43	2.144	12.8	33.8
Acetone	10.15	1.389	7.3	64.7
DMF	3.48	1.048	3.3	92.1
Dichloromethane	3.44	1.409	2.4	68.5
Acetonitrile	2.94	1.106	2.7	87.8

Parameters of quantum yields, fluorescence lifetimes, rate constants of radiative deactivation and non-radiative deactivation of **DSA-G⊂H2-2C4P** in different solvents ([**H2-2C4P**] = 50 μM, [**DSA-G**] = 100 μM).

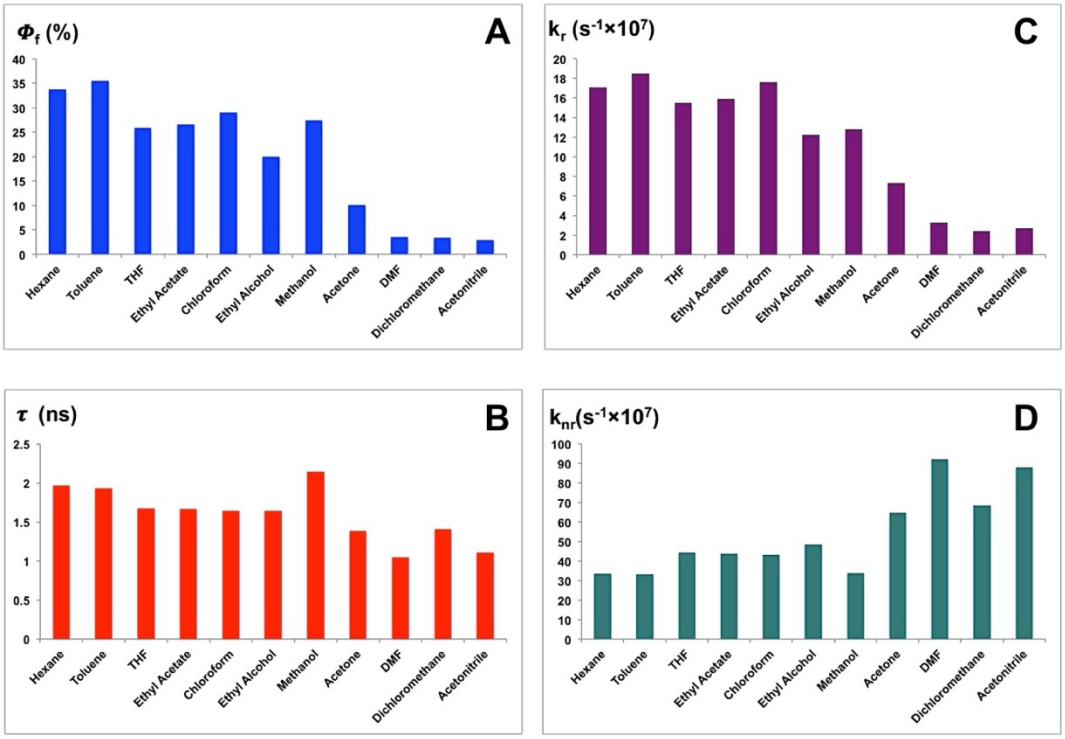

Figure S27. Quantum yields and time-resolved fluorescence decay curves. Histograms of (A) quantum yields, (B) rate constants of radiative deactivation, (C) fluorescence lifetimes and (D) rate constants of non-radiative deactivation of **DSA-G⊂H2-2C4P** in different solvents ([**H2-2C4P**] = 50 μM, [**DSA-G**] = 100 μM, as shown in Table S3).

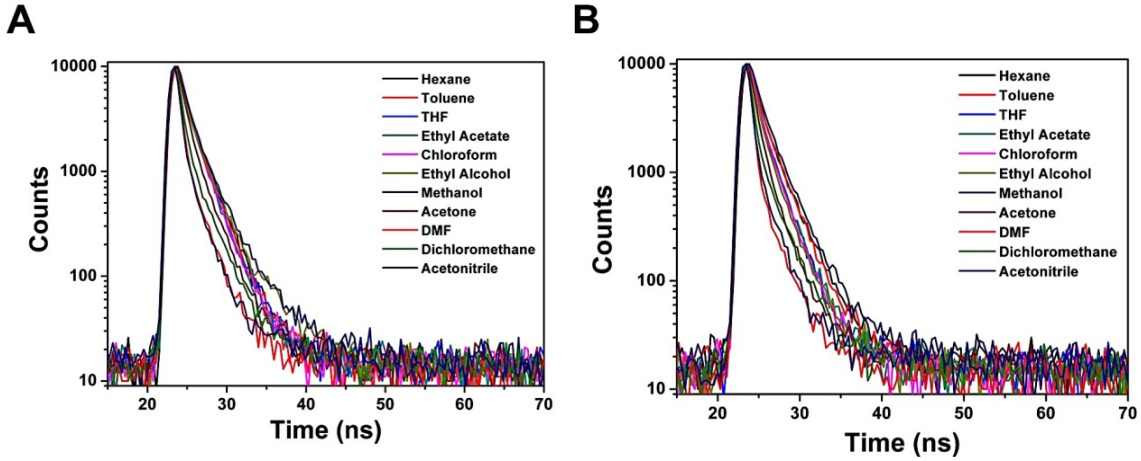

Figure S28. Time-resolved fluorescence decay curves. Time-resolved fluorescence decay curves of (A) **DSA-G⊂H1-4C4P** and (B) **DSA-G⊂H2-2C4P** in different solvents ([**H1-4C4P**] = 50 μM, [**H2-2C4P**] = 50 μM, [**DSA-G**] = 100 μM).

Table S4. Solid-state fluorescence Quantum Yields and Time-resolved Fluorescence Decay Curves

	Φ_f (%)	τ (ns)	k_r ($s^{-1}\times10^7$)	k_{nr} ($s^{-1}\times10^7$)
DSA-G	**18.12**	**1.438**	**12.6**	**56.9**
DSA-G⊂H1-4C4P	**68.68**	**3.214**	**21.4**	**1.0**
DSA-G⊂H2-2C4P	**56.18**	**3.004**	**18.7**	**14.6**

Parameters of quantum yields, fluorescence lifetimes, rate constants of radiative deactivation and non-radiative deactivation of individual **DSA-G, DSA-G⊂H1-4C4P** and **DSA-G⊂H2-2C4P** in the solid state.

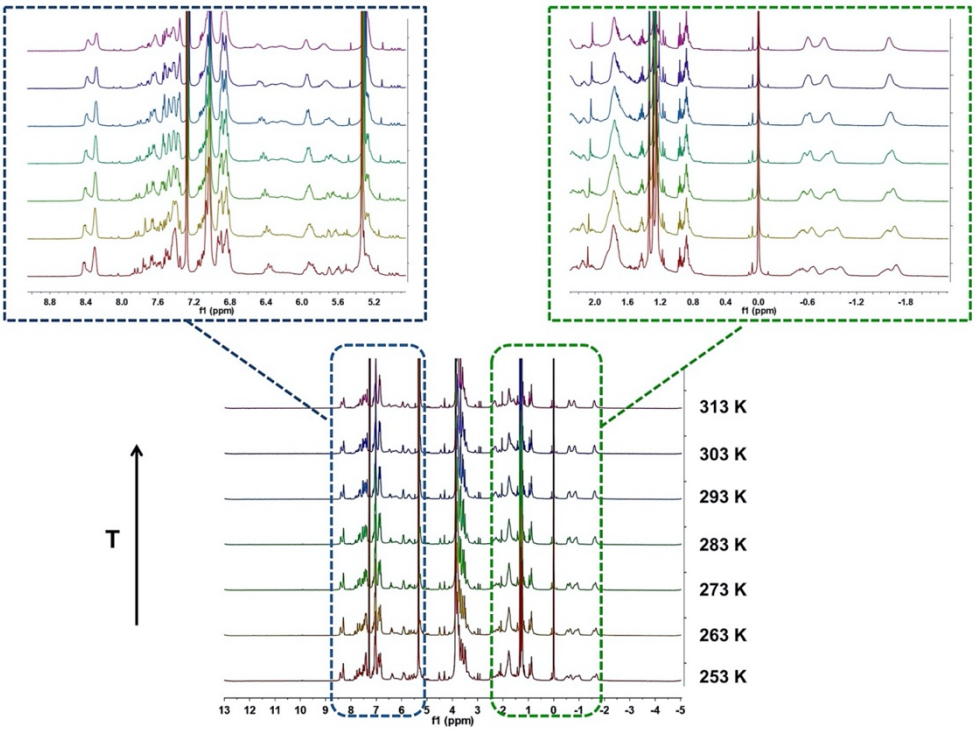

Figure S29. Variable-temperature NMR analysis. NMR spectra of **DSA-G⊂H1-4C4P** under temperature of 253 K, 263 K, 273 K, 283 K, 293 K, 303 K and 313 K ([**H1-4C4P**] = 2.0 mM, [**DSA-G**] = 1.0 mM; the analysis was performed with the temperature rising from the lowest to the highest values).

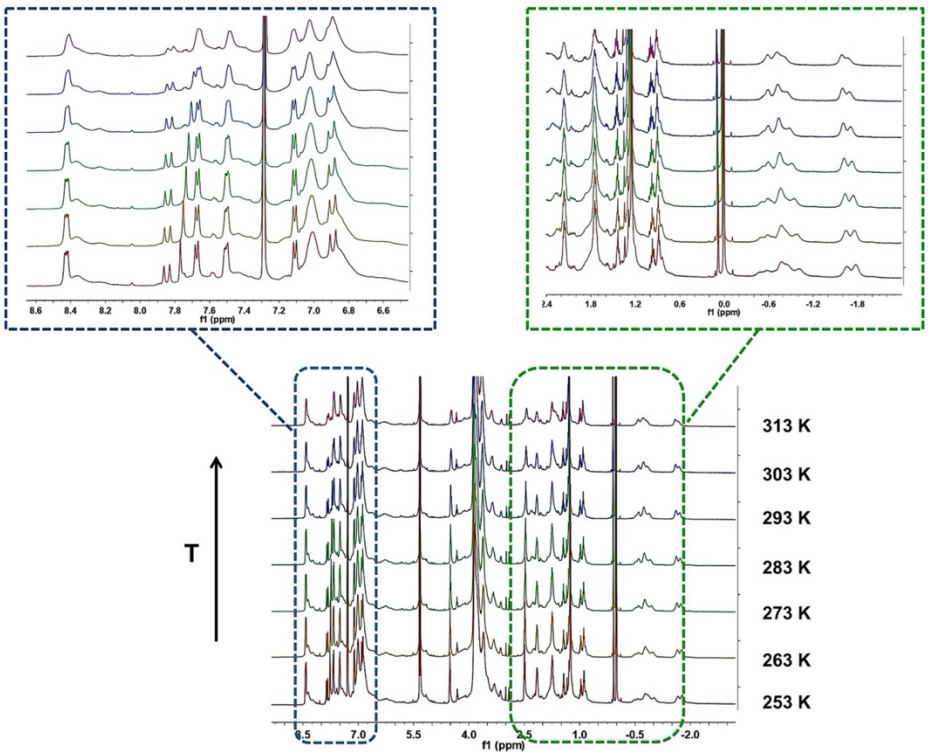

Figure S30. Variable-temperature NMR analysis. NMR spectra of **DSA-G⊂H2-2C4P** under temperature of 253 K, 263 K, 273 K, 283 K, 293 K, 303 K and 313 K ([**H2-2C4P**] = 2.0 mM, [**DSA-G**] = 1.0 mM; the analysis was performed with the temperature rising from the lowest to the highest values).

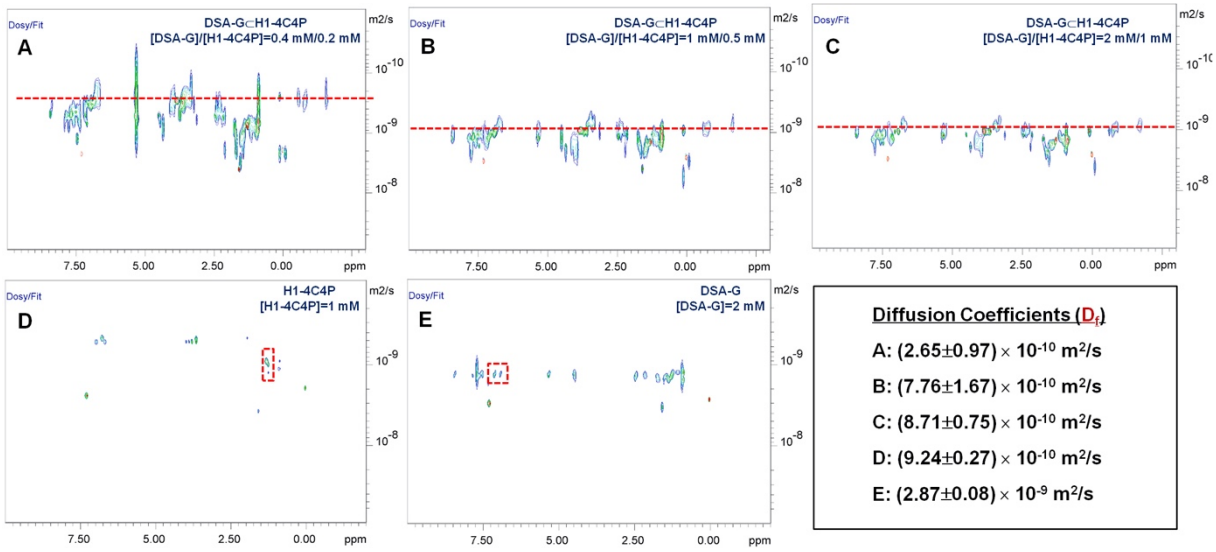

Figure S31. DOSY spectra of DSA-G⊂H1-4C4P at different concentration: (A) 0.4 mM/0.2 mM; (B) 1.0 mM/0.5 mM; (C) 2 mM/1 mM; (D) H1-4C4P; (E) DSA-G; The last box: diffusion coefficients of A, B, C, D, and E.

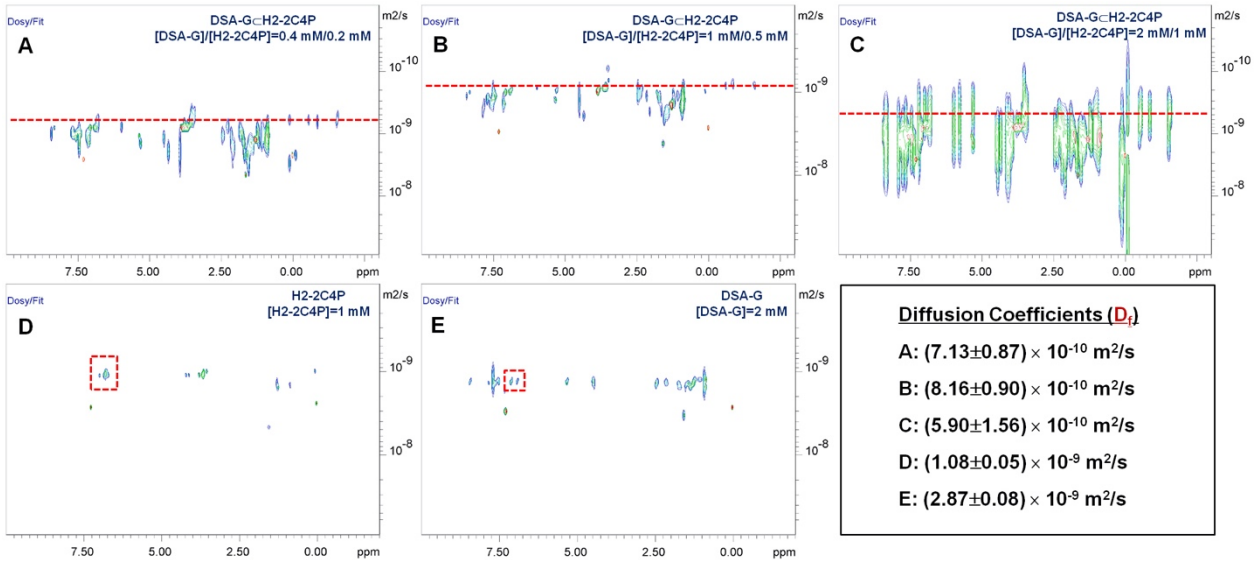

Figure S32. DOSY spectra of DSA-G⊂H2-2C4P at different concentration: (A) 0.4 mM/0.2 mM; (B) 1.0 mM/0.5 mM; (C) 2 mM/1 mM; (D) H2-2C4P; (E) DSA-G; The last box: diffusion coefficients of A, B, C, D, and E.

8. Fluorescence Microcopy Images of the Morphologies

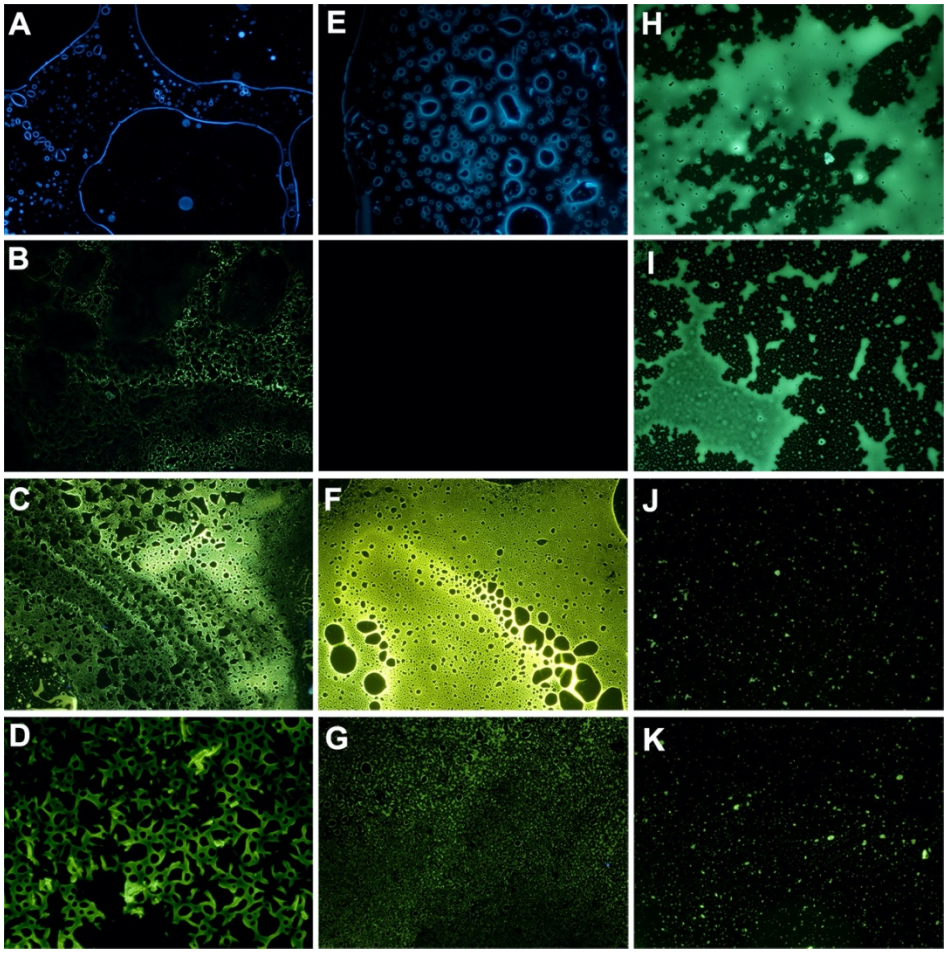

Figure S33. Fluorescence microscopy images. Fluorescence microscopy images of (A) **H1-4C4P** ([**H1-4C4P**] = 50 μM); (B) **DSA-G** ([**DSA-G**] = 100 μM); (C) **DSA-G⊂H1-4C4P** ([**H1-4C4P**] = 50 μM, [**DSA-G**] = 100 μM); (D) **DSA-G⊂H3-4C1P** ([**H3-4C1P**] = 200 μM, [**DSA-G**] = 100 μM); (E) **H2-2C4P** ([**H2-4C4**P] = 50 μM); (F) **DSA-G⊂H2-2C4P** ([**H2-2C4P**] = 50 μM, [**DSA-G**] = 100 μM); (G) **DSA-G⊂H4-2C1P** ([**H4-2C1P**] = 200 μM, [**DSA-G**] = 100 μM); (H) **DSA-G⊂H1-4C4P** ([**H1-4C4P**] = 50 μM, [**DSA-G**] = 10 μM); (I) **DSA-G⊂H2-2C4P** ([**H2-2C4P**] = 50 μM, [**DSA-G**] = 10 μM); (J) **DSA-G⊂H3-4C1P** ([**H3-4C1P**] = 100 μM, [**DSA-G**] = 100 μM); (K) **DSA-G⊂H4-2C1P** ([**H4-2C1P**] = 100 μM, [**DSA-G**] = 100 μM). (at a magnification of 20×, A-K: the same as in Figure 2). All of the samples are dried naturally from solution at room temperature.

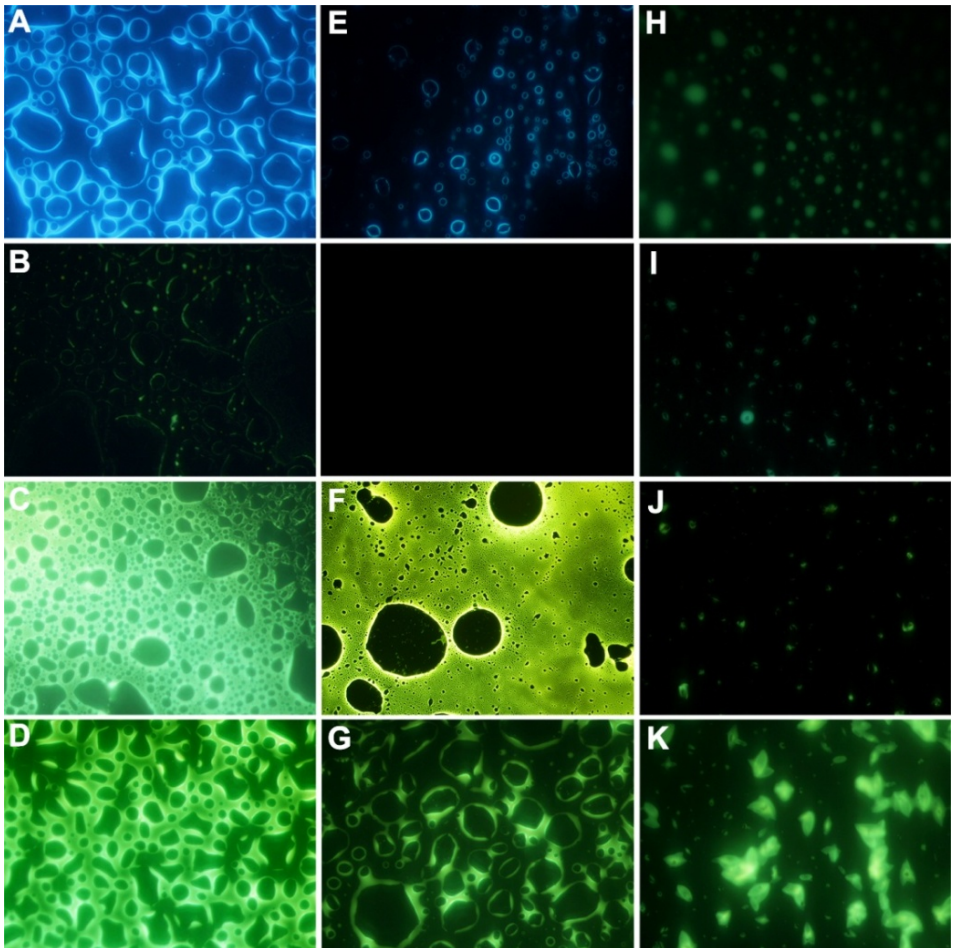

Figure S34. Fluorescence microscopy images. Fluorescence microscopy images of (A) **H1-4C4P** ([**H1-4C4P**] = 50 μM); (B) **DSA-G** ([**DSA-G**] = 100 μM); (C) **DSA-G⊂H1-4C4P** ([**H1-4C4P**] = 50 μM, [**DSA-G**] = 100 μM); (D) **DSA-G⊂H3-4C1P** ([**H3-4C1P**] = 200 μM, [**DSA-G**] = 100 μM); (E) **H2-2C4P** ([**H2-4C4P**] = 50 μM); (F) **DSA-G⊂H2-2C4P** ([**H2-2C4P**] = 50 μM, [**DSA-G**] = 100 μM); (G) **DSA-G⊂H4-2C1P** ([**H4-2C1P**] = 200 μM, [**DSA-G**] = 100 μM); (H) **DSA-G⊂H1-4C4P** ([**H1-4C4P**] = 50 μM, [**DSA-G**] = 10 μM); (I) **DSA-G⊂H2-2C4P** ([**H2-2C4P**] = 50 μM, [**DSA-G**] = 10 μM); (J) **DSA-G⊂H3-4C1P** ([**H3-4C1P**] = 100 μM, [**DSA-G**] = 100 μM); (K) **DSA-G⊂H4-2C1P** ([**H4-2C1P**] = 100 μM, [**DSA-G**] = 100 μM). (at a magnification of 100×, A-K: the same as in Figure 2). All of the samples are dried naturally from solution at room temperature.

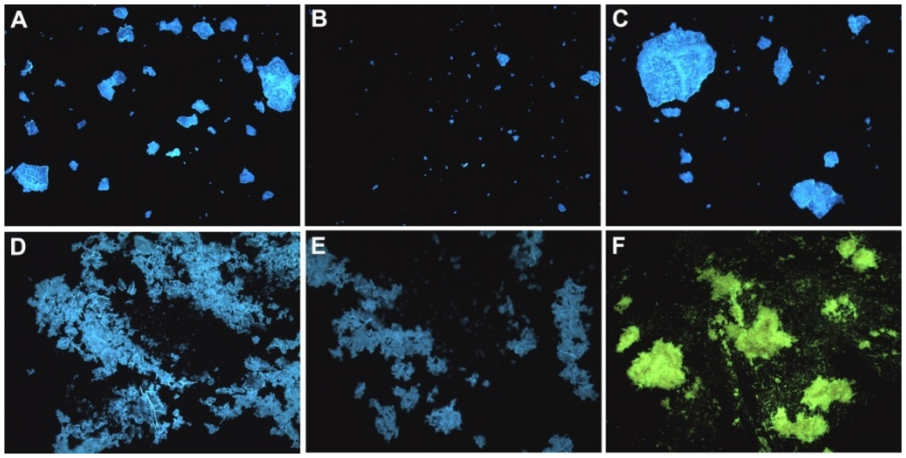

Figure S35. Fluorescence microscopy images of individual (A) **H1-4C4P**, (B and C) **H2-2C4P**, (D) **H3-4C1P**, (E) **H4-2C1P**, (F) **DSA-G (**at a magnification of 50×**)**.

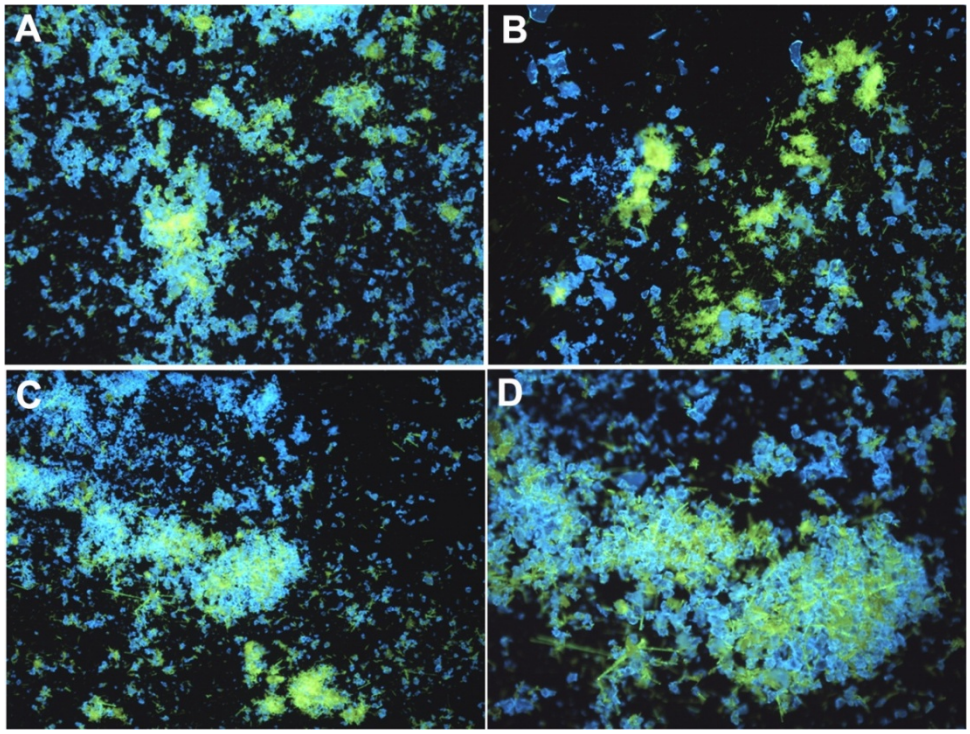

Figure S36. Fluorescence microscopy images of mechanically mixed (A and B) **DSA-G⊂H1-4C4P** and (C and D) **DSA-G⊂H2-2C4P (at a magnification of 50×)**.

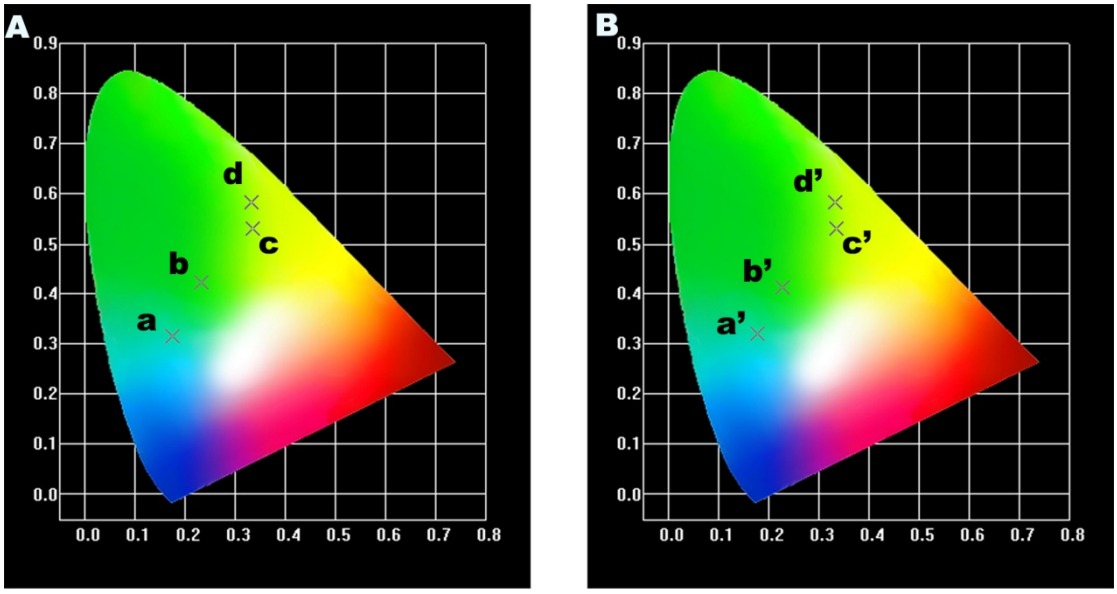

Figure S37. CIE chromaticity diagram of (A) DSA-G⊂H1-4C4P and (B) DSA-G⊂H2-2C4P (a: H1-4C4P; b: DSA-G⊂H1-4C4P (0.2:1); c: individual DSA-G; d: DSA-G⊂H1-4C4P (2:1); a': H2-2C4P; b': DSA-G⊂H2-2C4P (0.2:1); c': individual DSA-G; d': DSA-G⊂H2-2C4P (2:1)). CIE coordinates: a (0.1756, 0.3152), b (0.2323, 0.423), c (0.36, 0.5292), d (0.3322, 0.5819), a' (0.1773, 0.3192), b' (0.2263, 0.4116), c' (0.36, 0.5292), d' (0.3330, 0.5813).

9. References

[S1]N. Song, D.-X. Chen, Y.-C. Qiu, X.-Y. Yang, B. Xu, W. Tian and Y.-W. Yang, *Chem. Commun.,* 2014, **50**, 8231-8234.

[S2]N. Song, D.-X. Chen, M.-C. Xia, X.-L. Qiu, K. Ma, B. Xu, W. Tian and Y.-W. Yang, *Chem. Commun.,* 2015, **51**, 5526-5529.

[S3]X.-H. Wang, N. Song, W. Hou, C.-Y. Wang, Y. Wang, J. Tang and Y.-W. Yang, *Adv. Mater.,* 2019, **31**, 1903962.

[S4]X.-Y. Lou, N. Song and Y.-W. Yang, *Chem. Eur. J.,* 2019, **25**, 11975-11982.